Genomic and molecular characterisation of a *Klebsiella pneumoniae* clinical isolate resistant to meropenem-vaborbactam, imipenem-relebactam, and ceftazidime-avibactam

Yu Wan[1,2,3], Joshua L. C. Wong[4], Julia Sanchez-Garrido[4], Wen Wen Low[4], Jane F. Turton[1,5], Fabio Morecchiato[6], Ilaria Baccani[6], Kirsty Dodgson[8], Gian Maria Rossolini[6,7], Neil Woodford[5], Gad Frankel[4], Elita Jauneikaite[2], Danièle Meunier[1,5], and Katie L. Hopkins[1,2,5*]

[1] AMR & HCAI Division, UK Health Security Agency, London, United Kingdom

[2] NIHR Health Protection Research Unit in Healthcare Associated Infections and Antimicrobial Resistance, Department of Infectious Disease, Imperial College London, London, United Kingdom

[3] David Price Evans Global Health and Infectious Diseases Research Group, University of Liverpool, Liverpool, United Kingdom

[4] Department of Life Sciences, Imperial College London, London, United Kingdom

[5] Public Health Microbiology Reference Microbiology Division, UK Health Security Agency, London, United Kingdom

[6] Department of Experimental and Clinical Medicine, University of Florence, Florence, Italy

[7] Careggi University Hospital, Florence, Italy

[8] Department of Medical Microbiology, Manchester University NHS Foundation Trust, Manchester, United Kingdom

Address correspondence to Katie L. Hopkins (katie.hopkins@ukhsa.gov.uk)

Abstract

This article reports an unusual *Klebsiella pneumoniae* clinical isolate, KpMVR1, resistant to meropenem-vaborbactam, imipenem-relebactam, and ceftazidime-avibactam, and investigates the underlying genetic alterations using comparative genomics and molecular experiments.

Resistance to carbapenems and third-generation cephalosporins is increasing in *K. pneumoniae* globally, restricting therapeutic options. The β-lactam/β-lactamase inhibitor combinations are widely used to circumvent β-lactamase-mediated resistance. In 2021, isolate KpMVR1 was recovered from a hospitalised patient in England. Two additional isolates with the same variable-number tandem-repeat profile—KpMVS1, collected from the same patient 42 days before KpMVR1, and KpMVS2, from another patient in the same hospital—were susceptible to meropenem-vaborbactam, imipenem-relebactam, and ceftazidime-avibactam. Illumina and nanopore whole-genome sequencing and hybrid genome assembly were conducted for these three isolates. Annotated genome assemblies were compared to identify genetic variation, and mutagenesis experiments were performed to verify predicted functional alterations.

All isolates belonged to a novel clone ST8134 and carried $bla_{\text{KPC-2}}$-like alleles (KpMVR1: $bla_{\text{KPC-157}}$; KpMVS1 and KpMVS2: $bla_{\text{KPC-2}}$) in presumptively conjugative plasmids. IS*Ec68* caused a frameshift mutation in KpMVR1's *ompK36* gene, reducing the meropenem-vaborbactam and imipenem-relebactam susceptibility. KPC-157 demonstrated decreased hydrolysis of imipenem and ceftazidime when compared with KPC-2. KpMVR1 also encoded a disrupted transcriptional repressor MarR and a destabilising mutation in AcrB, a component of the AcrAB-TolC multidrug efflux pump. In conclusion, KpMVR1 harboured complex resistance-associated genetic alterations, with evidence for *in vivo* emergence of antimicrobial resistance. Our study underlines routine screening for resistant pathogens in vulnerable patients to guide antimicrobial chemotherapy as well as the need to characterise underlying resistance mechanisms to help assess the potential for onward transmission.

Keywords

Klebsiella pneumoniae, antimicrobial resistance, combination antimicrobials, β-lactam antimicrobials, β-lactamase inhibitors, porins, medical microbiology, bioinformatics, comparative genomics, mutagenesis experiments

Data summary

Illumina and nanopore sequencing reads, hybrid genome assemblies, and anonymised metadata of isolates KpMVS1, KpMVR1, and KpMVS2 have been deposited in databases of the National Center for Biotechnology Information (www.ncbi.nlm.nih.gov) under BioProject accession PRJNA1084250, with BioSample accessions SAMN46778009 (KpMVS1), SAMN46778010 (KpMVR1), and SAMN46778011 (KpMVS2). The genome assemblies of these isolates have also been deposited in Pasteur Institute's database for *K. pneumoniae* species complex (bigsdb.pasteur.fr/klebsiella/) under ids 75608 (KpMVS1), 75609 (KpMVR1), and 75610 (KpMVS2).

Impact statement

This is the first bla_{KPC}-positive *K. pneumoniae* isolate referred to the UK's national reference laboratory with resistance to three last-resort β-lactam/β-lactamase inhibitor combinations meropenem-vaborbactam, imipenem-relebactam, and ceftazidime-avibactam, implicating *in vivo* emergence of this unusual resistance profile during prolonged antimicrobial chemotherapy. This isolate belonged to a novel clone ST8134 and harboured a plasmid-borne bla_{KPC-2}-like allele $bla_{KPC-157}$. We identified complex genetic alterations in this isolate: chromosomal large deletions, point mutations, and an IS*Ec68*-induced loss-of-function truncation of the *ompK36* porin gene. We determined the impact of KPC-2, KPC-157, and the *ompK36* truncation on the susceptibility of *K. pneumoniae* to meropenem, meropenem-vaborbactam, imipenem, imipenem-relebactam, imipenem-avibactam, aztreonam, aztreonam-avibactam, ceftazidime, ceftazidime-avibactam, and cefiderocol.

69 Our work underscores the need to monitor emerging resistance to beta-lactam/beta-lactamase inhibitor
70 combinations in healthcare and to understand underlying resistance mechanisms for assessing the
71 potential of pathogen transmission.

72 ## Introduction

73 Meropenem and imipenem are broad-spectrum carbapenem antimicrobials parenterally administrated
74 to treat serious bacterial infections, such as those caused by Enterobacterales producing extended-
75 spectrum β-lactamases (ESBLs) or AmpC-type cephalosporinases (AmpCs) [1–3]. Ceftazidime, a
76 third-generation parenteral cephalosporin, is also widely used for treating severe bacterial infections,
77 although it can be hydrolysed by ESBLs and AmpCs [4, 5]. In Gram-negative bacteria, carbapenems
78 and cephalosporins diffuse through outer-membrane porins and enter the periplasm, where they
79 inactivate penicillin binding proteins, disrupting cell-wall synthesis with a bactericidal effect [6–8].

80 Combining β-lactams with β-lactamase inhibitors in antimicrobial chemotherapy is a widely
81 employed strategy to circumvent β-lactamase-mediated resistance in bacteria. Vaborbactam,
82 relebactam, and avibactam are non-β-lactam inhibitors of Ambler class A β-lactamases, such as ESBLs
83 and *Klebsiella pneumoniae* carbapenemases (KPCs), as well as class C β-lactamases (AmpCs) [9].
84 Moreover, avibactam inhibits several class D β-lactamases such as OXA-48 and OXA-10 [10]. These
85 inhibitors penetrate the outer membrane (OM) of Gram-negative bacteria via porins, blocking the
86 active sites of β-lactamases in the periplasm [9, 11].

87 In the UK, meropenem-vaborbactam, imipenem-relebactam, and ceftazidime-avibactam are
88 reserved for highly selected patients [12]. Resistance to one or more of these combination
89 antimicrobials in clinical isolates of KPC-producing *Klebsiella pneumoniae* has been previously
90 reported [13–15]. Underlying resistance mechanisms include overproduction of KPCs or the AcrAB-
91 TolC multidrug efflux pump, as well as gain-of-function point mutations in the bla_{KPC} gene [9, 16–
92 18]. In addition, the disruption or transcriptional downregulation of *ompK35* (*ompF*) and *ompK36*
93 (*ompC*), which encode non-selective porins that facilitate the diffusion of β-lactams and β-lactamase
94 inhibitors through the OM, has also been implicated [17–20].

95 Here, we report and characterise a clinically significant *K. pneumoniae* isolate exhibiting resistance
96 to ceftazidime-avibactam, meropenem-vaborbactam, and imipenem-relebactam, analysed in the

97 context of closely related isolates recovered in the same hospital. This was the first such isolate referred
98 to the UK's national reference laboratory for characterisation.

99 Methods

100 Isolate collection and phenotyping

101 The *K. pneumoniae* isolate KpMVS1 was recovered from a lung biopsy specimen of an inpatient
102 (hereafter, Patient 1) admitted to an intensive care unit (ICU) in England in 2021. The second *K.*
103 *pneumoniae* isolate, KpMVR1, was recovered from a groin wound of the same patient 42 days later.
104 During this ICU stay, the patient received a broad range of antimicrobials, including meropenem-
105 vaborbactam, ciprofloxacin, and gentamicin; however, ceftazidime-avibactam and imipenem-
106 relebactam were not used.

107 Species identification of the isolates and carbapenemase gene screening were performed using
108 matrix-assisted laser desorption/ionisation-time of flight (MALDI-ToF) method and the GeneXpert
109 system (Cepheid, USA), respectively. Initial antimicrobial susceptibility testing (AST) was conducted
110 by the hospital, with results interpreted according to the European Committee on Antimicrobial
111 Susceptibility Testing (EUCAST) guidelines. Both isolates were referred to the Antimicrobial
112 Resistance and Healthcare Associated Infections (AMRHAI) Reference Unit of the UK Health
113 Security Agency (UKHSA) for variable number tandem repeat (VNTR) typing [21] and investigation
114 of unusual antimicrobial resistance (AMR). Furthermore, a bla_{KPC}-positive *K. pneumoniae* isolate
115 KpMVS2 — recovered from a rectal swab of another patient (Patient 2) in the same hospital in 2020
116 during an outbreak investigation and sharing the same VNTR profile as KpMVS1 and KpMVR1 —
117 was retrieved from AMRHAI's culture collection for comparison. These three isolates were subjected
118 to whole-genome sequencing (WGS) and AST for which minimum inhibitory concentrations (MICs)
119 of 19 antimicrobials (Table 1) and diameters of cefiderocol inhibition zones were interpreted as per
120 EUCAST clinical breakpoints v15.0 [22].

121 **Whole-genome sequencing**

122 Genomic DNA of each isolate was extracted from an overnight culture using the GeneJET Kit
123 (ThermoFisher Scientific, UK) as per the manufacturer's protocol. Short-read sequencing was
124 conducted on a HiSeq 2500 system (Illumina, USA) by UKHSA's Colindale Sequencing Laboratory
125 following its paired-end 101-bp protocol. Long-read sequencing was performed on MinION R9.4.1
126 flow cells (Oxford Nanopore Technologies [ONT], UK), with libraries prepared using the ONT Rapid
127 Barcoding Kit SQK-RBK004.

128 **Bioinformatics analysis**

129 Illumina reads were trimmed and filtered with Trimmomatic v0.39 for a minimum per-read quality of
130 Phred Q30 and minimum length of 50 bp [23]. Fast-mode basecalling and de-multiplexing of nanopore
131 reads was conducted by guppy v4 (ONT). Nanopore reads were then trimmed and filtered for a
132 minimum per-read quality of Q10 and minimum length of 1 kbp using fastp v0.23.4 [24]. For species
133 confirmation and contamination assessment, taxonomical profiling of processed Illumina and
134 nanopore reads were performed using Kraken v2.1.3, bracken v2.8, and a standard Kraken database
135 built in September 2023 [25, 26].

136 Genomes of KpMVR1 and KpMVS2, with estimated nanopore read depths of 185× and 243×,
137 respectively, were assembled using hybracter v0.5.0 (assemblers: Flye v2.9.3 and plassembler v1.5.0;
138 sequence re-orientator: dnaapler v0.5.1; long-read polisher: medaka v1.8.0, short-read polishers:
139 pypolca v0.2.1 and polypolish v0.5.0) [27–32]. For KpMVS1, which had nanopore reads with an
140 estimated depth of 64×, the chromosome and plasmid sequences were assembled using Raven v1.8.3
141 and plassembler, respectively, and polished with nanopore and Illumina reads as for KpMVR1 and
142 KpMVS2. Evaluation of contamination and completeness of genome assemblies were conducted with
143 CheckM2 v1.0.2 and its database Uniref100/KO [33]. The average fold-coverage of each contig was
144 estimated from Illumina and nanopore reads, respectively, using mosdepth v0.3.9 [34].

145 The genome assemblies were annotated using bakta v1.9.2 and its standard database v5.1 [35].
146 Multi-locus sequence typing, serotype prediction, and virulence-factor detection were performed using
147 Kleborate v3.1.3, which incorporated Kaptive v3.1.0 [36, 37]. AMR genes were detected using
148 AMRFinderPlus v3.12.8 with a minimum query coverage of 80% [38]. Clustered regularly interspaced
149 short palindromic repeats (CRISPR) and CRISPR-associated (Cas) genes in chromosomes were
150 predicted using CRISPRCasFinder [39]. For plasmids, replicon types were determined at a minimum
151 of 80% nucleotide identity and coverage using PlasmidFinder v2.1 [40] and the mobility was predicted
152 using mob_typer of MOB-suite v3.1.8 [41]. The fold-coverage of each KPC-encoding plasmid was
153 divided by that of its host's chromosome to estimate the plasmid copy number. Transposons and
154 insertion sequences (ISs) were identified using TnCentral Blast (blastn) and ISFinder, respectively [42,
155 43].
156 Chromosome and plasmids of KpMVR1 and KpMVS2 were compared against those of KpMVS1
157 using minimap v2.26 [44]. Identified genetic variants were annotated using snpEff v5.2 [45]. Gene
158 Ontology terms were predicted from amino acid sequences using InterProScan v5.69-101.0 [46] with
159 sequence alignments filtered for ≥60% query coverages. Impacts of point mutations on protein stability
160 were predicted from wild-type protein structures in the UniProt database using Missense3D and
161 DDMut [47–49]. The three-dimensional structure of the plasmid-encoded donor OM protein TraN was
162 compared between KPC-encoding, IncFII-carrying plasmids pKpMVS1_1, pKpMVR1_1, and
163 pKpMVS2_1 following the approach developed by Low *et al* (Supplementary methods) to estimate
164 the impact of TraN alterations on the conjugation specificity and efficiency [50]. Comparison and
165 annotations of these three plasmids were visualised using BRIG v0.95 and Proksee [51, 52]. Gene
166 synteny was illustrated using R package gggenes [53]. Genetic alterations found in both KpMVR1 and
167 KpMVS2 were considered unlikely to confer the unique AMR profiles of KpMVR1 and were therefore
168 excluded from further investigation.

169 **Functional assessment**

170 To experimentally determine and compare the impacts of *bla*$_{KPC-2}$ and *bla*$_{KPC-157}$ on β-lactam
171 susceptibility in *K. pneumoniae*, KpMVS1's KPC-2-encoding plasmid pKpMVS1_1, was introduced
172 into the plasmid-free *K. pneumoniae* laboratory strain ICC8001 (MICs: meropenem, ≤0.06 mg/L;
173 imipenem, 0.25 mg/L; aztreonam, ≤0.125 mg/L; ceftazidime and ceftazidime-avibactam, 0.25 mg/L)
174 through conjugation, resulting in a transconjugant ICC8001$_{KPC-2}$ [54]. Transgenic isolates
175 ICC8001$_{KPC-157}$ and KpMVS1$_{KPC-157}$ were derived from ICC8001$_{KPC-2}$ and KpMVS1, respectively, by
176 substituting the *bla*$_{KPC-2}$ allele with *bla*$_{KPC-157}$. Moreover, isolates ICC8001$_{KPC-2/\Delta ompK36}$ and ICC8001$_{KPC-}$
177 $_{157/\Delta ompK36}$ were derived from ICC8001$_{KPC-2}$ and ICC8001$_{KPC-157}$, respectively, through seamless,
178 markerless homologous recombination using mutagenesis vectors and a lambda-red based
179 recombination system generated in previous work [54].

180 To predict the presence/absence of OmpK36 in the OM of KpMVR1, Sec-dependent signal
181 peptides and their cleavage site in translated *ompK36* alleles were compared between KpMVS1 and
182 KpMVR1 using SignalP v6.0 [55]. To validate the prediction, purification of OM proteins was
183 performed by resuspending an overnight LB-Miller culture (VWR, USA) of each isolate in 1M HEPES
184 (pH 7.4) and sonicating at 25% amplitude for 10 bursts of 10 seconds on, 15 seconds off each (Model
185 705 Sonic Dismembrator, Fisher Scientific). Isolates ICC8001 and its *ompK36*-knockout derivative,
186 ICC8001$_{\Delta ompK36}$, were included as positive and negative controls, respectively. After separating
187 cellular debris by centrifugation, OM proteins were obtained by centrifugation at 14,000×g for 30 mins
188 and resuspended in 2% sarcosine/HEPES for 30 mins at room temperature. All steps were performed
189 at 4°C on ice to preserve protein integrity unless otherwise indicated. For visualisation, 10 μg protein
190 per isolate was separated by sodium dodecyl sulfate–polyacrylamide gel electrophoresis (SDS-PAGE)
191 using 12% acrylamide gels and was stained with Coomassie solution (Sigma-Aldrich, USA) and
192 imaged on a ChemiDoc XRS+ (Bio-Rad, USA).

193 Both progenitor isolates (KpMVS1 and KpMVR1) and the five transgenic isolates (KpMVS1$_{KPC-157}$, ICC8001$_{KPC-2}$, ICC8001$_{KPC-157}$, ICC8001$_{KPC-2/\Delta ompK36}$, and ICC8001$_{KPC-157/\Delta ompK36}$) were tested for susceptibility to meropenem, meropenem-vaborbactam, imipenem, imipenem-relebactam, imipenem-avibactam, ceftazidime, ceftazidime-avibactam, aztreonam, aztreonam-avibactam, and cefiderocol (in iron-depleted medium) by the reference broth microdilution method as per the EUCAST guidance [56, 57]. Any MIC change above a two-fold difference between two isolates was considered notable.

Results

Phenotypes of isolates

Isolates KpMVS1 and KpMVR1, obtained 42 days apart from Patient 1 with recurrent *K. pneumoniae* infections, and KpMVS2, obtained from Patient 2 in the same hospital, were identified as *K. pneumoniae* by both MALDI-ToF and WGS. In the ICU where KpMVS1 and KpMVR1 were recovered, all patients were screened for carriage of carbapenemase-producing Enterobacterales (CPE) on admission using PCR, and the resistance profile of KpMVR1 was unique among all identified CPE isolates from the ICU during Patient 1's stay.

Based on AST results from the AMRHAI Reference Unit (Table 1), KpMVR1 was resistant to meropenem-vaborbactam (MIC>256 mg/L), ceftazidime-avibactam (MIC=16 mg/L), and ciprofloxacin (MIC>4 mg/L), whereas KpMVS1 and KpMVS2 were susceptible to these antimicrobial agents (MICs: meropenem-vaborbactam ≤0.064 mg/L; ceftazidime-avibactam 1 mg/L; ciprofloxacin ≤0.125 mg/L). Notably, KpMVS2 was resistant to cefiderocol. Further AST discovered that the imipenem-relebactam MIC of KpMVR1 (512 mg/L, resistant) was 2048 times that of KpMVS1 (0.25 mg/L, susceptible) (Table 2). Moreover, KpMVR1 exhibited a >4-fold increase in the temocillin MIC (>128 mg/L) and a >8-fold reduction in the cefepime MIC (4 mg/L, susceptible, increased exposure) compared with KpMVS1 (temocillin: 32 mg/L; cefepime: >32 mg/L, resistant).

216 **Table 1.** Antimicrobial minimum inhibitory concentrations (MICs; mg/L) determined by UKHSA's AMRHAI Reference Unit and susceptibility interpretations
217 (as per EUCAST clinical breakpoints v15.0) of three *K. pneumoniae* clinical isolates. Abbreviations: MEM, meropenem; VAB, vaborbactam; IPM, imipenem;
218 ETP, ertapenem; CET, ceftolozane; TZB, tazobactam; CFD, cefiderocol; FEP, cefepime; CAZ, ceftazidime; AVI, avibactam; CTX, cefotaxime; FOX, cefoxitin;
219 TMC, temocillin; AMP, ampicillin; AMX, amoxicillin; CAV, clavulanate; PIP, piperacillin; ATM, aztreonam; AMK, amikacin; GEN, gentamicin; CST, colistin;
220 CIP, ciprofloxacin; MB, monobactam. Susceptibility interpretations: R, resistant; I, susceptible, increased exposure; S, susceptible.

	Carbapenem				**Cephalosporin**							**Penicillin**				**MB**	**Aminoglycoside**		**Others**	
Isolate	**MEM-VAB**	**MEM**	**IPM**	**ETP**	**CET-TZB**	**CFD***	**FEP**	**CAZ**	**CAZ-AVI**	**CTX**	**FOX‡**	**TMC‡**	**AMP**	**AMX-CAV**	**PIP-TZB**	**ATM**	**AMK‡**	**GEN‡**	**CST‡**	**CIP**
KpMVR1	>256 (R)	>16 (R)	>128 (R)	>4 (R)	16 (R)	(S)	4 (I)	256 (R)	16 (R)	8 (R)	>64	>128	>32 (R)	>32 (R)	>64 (R)	16 (R)	2	0.5	≤0.5	>4 (R)
KpMVS1	0.064 (S)	>16 (R)	64 (R)	>4 (R)	>16 (R)	(S)	>32 (R)	128 (R)	1 (S)	64 (R)	>64	32	>32 (R)	>32 (R)	>64 (R)	>32 (R)	≤1	≤0.25	≤0.5	≤0.125 (S)
KpMVS2	0.032 (S)	16 (R)	16 (R)	>4 (R)	>16 (R)	(R)	>32 (R)	64 (R)	1 (S)	16 (R)	32	8	>32 (R)	>32 (R)	>64 (R)	>32 (R)	≤1	≤0.25	1	≤0.125 (S)

221 * CFD susceptibility was determined using disc diffusion. ‡ Interpretations were not available according to EUCAST guidelines.

222

223 **Table 2.** Minimum inhibitory concentrations of beta-lactam antimicrobials and susceptibility interpretations (as per EUCAST clinical breakpoints v15.0, where
224 applicable) of progenitor and transgenic *K. pneumoniae* isolates determined in the experiments for functional assessment. Subscripts in isolate names indicate
225 transgenic isolates and corresponding genotypes. Abbreviations: MEM, meropenem; VAB, vaborbactam; IPM, imipenem; REL, relebactam; ATM, aztreonam;
226 AVI, avibactam; CAZ, ceftazidime; CFD, cefiderocol, tested in iron-depleted Mueller Hinton broth; NT, not tested. Interpretations of antimicrobial susceptibility:
227 R, resistant; I, susceptible upon increased antimicrobial exposure; S, susceptible. Notations: *ompK36*fs, frameshifted *ompK36*; Δ*ompK36*, deletion of *ompK36*.

Isolate	**Genotype**		**Minimum Inhibitory Concentration (mg/L) and interpretation**									
			MEM	**MEM-VAB**	**IPM**	**IPM-REL**	**IPM-AVI**	**ATM**	**ATM-AVI**	**CAZ**	**CAZ-AVI**	**CFD**
KpMVR1	$bla_{KPC-157}$	*ompK36*fs	512 (R)	256 (R)	512 (R)	512 (R)	NT	16 (R)	4 (S)	8 (R)	8 (S)	0.5 (S)
KpMVS1	bla_{KPC-2}	*ompK36*	32 (R)	≤0.06 (S)	32 (R)	0.25 (S)	≤0.5	512 (R)	0.25 (S)	32 (R)	0.5 (S)	0.25 (S)
$KpMVS1_{KPC-157}$	$bla_{KPC-157}$	*ompK36*	16 (R)	≤0.06 (S)	8 (R)	8 (R)	≤0.5	2 (I)	0.25 (S)	1 (S)	0.25 (S)	≤0.06 (S)
$ICC8001_{KPC-2}$	bla_{KPC-2}	*ompK36*	16 (R)	≤0.06 (S)	16 (R)	0.25 (S)	≤0.5	512 (R)	0.125 (S)	32 (R)	0.25 (S)	0.25 (S)
$ICC8001_{KPC-157}$	$bla_{KPC-157}$	*ompK36*	16 (R)	≤0.06 (S)	4 (I)	4 (R)	≤0.5	1 (S)	0.125 (S)	0.5 (S)	0.125 (S)	≤0.06 (S)
$ICC8001_{KPC-2/\Delta ompK36}$	bla_{KPC-2}	Δ*ompK36*	256 (R)	2 (S)	256 (R)	2 (S)	NT	>1024 (R)	0.25 (S)	16 (R)	0.5 (S)	0.25 (S)
$ICC8001_{KPC-157/\Delta ompK36}$	$bla_{KPC-157}$	Δ*ompK36*	256 (R)	4 (S)	256 (R)	128 (R)	NT	4 (I)	0.25 (S)	1 (S)	0.5 (S)	0.25 (S)

228

229

230 **Table 3.** Genetic characteristics of the three *K. pneumoniae* clinical isolates. Abbreviation: AMR, antimicrobial resistance. Each hit of plasmid replicons covered
231 the full length of its reference sequence in the PlasmidFinder database.

Isolate	Sequence	Category	Length (bp)	Plasmid type	Nucleotide identity to template	Plasmid mobility	AMR gene
KpMVS1	KpMVS1	Chromosome	5,404,514				$bla_{\text{SHV-36}}$, *fosA10*
	pKpMVS1_1	Plasmid	111,397	IncFII/repB(R1701)	IncFII(pKP91): 100%; repB(R1701): 99.52%	Conjugative	$bla_{\text{KPC-2}}$
	pKpMVS1_2	Plasmid	41,868	IncFII(pMET)	IncFII(pMET): 98.09%	Non-mobilisable	
	pKpMVS1_3	Plasmid	4,809	Col(pHAD28)	Col(pHAD28): 92.37%	Non-mobilisable	
	pKpMVS1_4	Plasmid	4,439	Col(pHAD28)/Col440II	Col(pHAD28): 93.13%; Col440II: 97.52%	Mobilisable	
	pKpMVS1_5	Plasmid	3,258	Unknown	Not detected	Non-mobilisable	
	pKpMVS1_6	Plasmid	1,917	Col(pHAD28)	Col(pHAD28): 100%	Mobilisable	
KpMVR1	KpMVR1	Chromosome	5,292,801				$bla_{\text{SHV-36}}$, *fosA10*
	pKpMVR1_1	Plasmid	111,174	IncFII/repB(R1701)	IncFII(pKP91): 100%, repB(R1701): 99.52%	Conjugative	$bla_{\text{KPC-157}}$
	pKpMVR1_2	Plasmid	41,868	IncFII(pMET)	IncFII(pMET): 98.09%	Non-mobilisable	
	pKpMVR1_3	Plasmid	4,809	Col(pHAD28)	Col(pHAD28): 92.37%	Non-mobilisable	
	pKpMVR1_4	Plasmid	4,439	Col(pHAD28)/Col440II	Col(pHAD28): 93.13%; Col440II: 97.52%	Mobilisable	
	pKpMVR1_5	Plasmid	3,258	Unknown	Not detected	Non-mobilisable	
	pKpMVR1_6	Plasmid	1,917	Col(pHAD28)	Col (pHAD28): 100%	Mobilisable	
KpMVS2	KpMVS2	Chromosome	5,354,507				$bla_{\text{SHV-36}}$, *fosA10*
	pKpMVS2_1	Plasmid	116,795	IncFII/IncR	IncFII(pKP91): 100%; IncR: 99.6%	Conjugative	$bla_{\text{KPC-2}}$
	pKpMVS2_2	Plasmid	41,868	IncFII(pMET)	IncFII(pMET): 98.09%	Non-mobilisable	
	pKpMVS2_3	Plasmid	4,808	Col(pHAD28)	Col (pHAD28): 92.37%*	Non-mobilisable	
	pKpMVS2_4	Plasmid	4,187	Col(pHAD28)	Col (pHAD28): 92.37%*	Non-mobilisable	
	pKpMVS2_5	Plasmid	3,258	Unknown	Not detected	Non-mobilisable	
	pKpMVS2_6	Plasmid	1,917	Col(pHAD28)	Col (pHAD28): 100%	Mobilisable	
	pKpMVS2_7	Plasmid	240,297	IncFII(pKP91)/IncFIB(K)	IncFII(pKP91): 84.98%; IncFIB(K): 98.93%	Conjugative	

232 * Two hits of the Col(pHAD28) template sequence in the PlasmidFinder database differed between pKpMVS2_3 and pKpMVS2_4 by seven nucleotide
233 substitutions (95% nucleotide identity) despite their same percent identity to the template.

234 **Table 4.** Chromosomal genetic variation in isolate KpMVR1 identified via comparison against its progenitor KpMVS1. Coordinates refer to locations in the
235 reference sequence of the KpMVS1 chromosome. Variants shared by both KpMVR1 and KpMVS2 against their common reference sequence of KpMVS1 are
236 indicated by asterisks following the coordinates. The "^" sign indicates an insertion between two consecutive bases in the reference sequence. Abbreviations:
237 CRISPR, clustered regularly interspaced short palindromic repeats; Cas: CRISPR-associated genes; Del, deletion; Ins, insertion; fs, frameshift.

Location	Locus	Product	Variant type	DNA change	Protein change
455179	*rrl*	23S rRNA	Substitution	G>T	
1050491 – 1070213	Multiple	Type I-E CRISPR-Cas system, *etc*. (Figure S3, Table S3)	Deletion	Deletion of 19,723 bp	Loss of production
1113441 – 1113446	*flhA*	Formate hydrogenlyase transcriptional activator	Deletion	Deletion of 6 bp	L367Del, T368Del
1218110^1218111 *	*rrl*	23S rRNA	Insertion	Insertion of base G	
1578603	*gyrA*	DNA topoisomerase (ATP-hydrolyzing) subunit A	Substitution	248C>A	S83Y
1588108^1588109	*ompK36*	Outer membrane porin OmpK36	Insertion	Insertion of IS*Ec68*	Amino acid substitutions
1724677^1724678 *	*xylB*	Xylulose kinase	Insertion	Insertion of base G	I236fs
1792900	*rfbD*	UDP-galactopyranose mutase	Substitution	578T>A	M193K
1819375^1819376	Intergenic		Insertion	Insertion of base C	
2183835^2183836 *	Intergenic		Insertion	Insertion of base T	
2183837 *	Intergenic		Substitution	A>T	
2201799–2256547	Multiple	Multiple products including transporters (Figure 1, Table S2)	Deletion	Deletion of 54,749 bp	Loss of production
2759671–2759685	*marR*	Multiple-AMR (Mar) transcriptional repressor MarR	Deletion	Deletion of bases 263–277	P88–D92Del, K93Q
3157221^3157222 *	Intergenic		Insertion	Insertion of base C	
3189754 – 3223285 *	Multiple	Multiple products (Figure S4, Table S4)	Deletion	Deletion of 33,532 bp	Loss of production
3274833	*phoQ*	Two-component system sensor histidine kinase	Substitution	C>T	T156I
3580334 – 3585227 *	Multiple	IS*3H* composite transposon (Figure S5, Table S5)	Deletion	Deletion of 4,894 bp	Loss of production
4104884	*acrB*	Multidrug efflux RND transporter permease subunit AcrB	Substitution	T>G	L667R
4262704^ 4262705	*ecpR*	Regulator protein EcpR	Insertion	Insertion (2 bp)	I115fs
4723928	*rrl*	23S ribosomal RNA	Deletion	Deletion of base C	
5349457	*rrl*	23S ribosomal RNA	Deletion	Deletion of base C	

238

239 **Genetic characteristics of isolates**

240 All three isolates belonged to *K. pneumoniae* clone ST8134, a novel single-locus variant of ST240,
241 and were predicted to share the O1αβ,2β O-antigen type and K62 capsular polysaccharide type.
242 Sequence lengths, plasmid replicons, and AMR genes determined in hybrid genome assemblies are
243 summarised in Table 3. KpMVR1 and KpMVS1 shared the same plasmid types IncFII/repB(R1701),
244 IncFII(pMET), Col(pHAD28), and Col(pHAD28)/Col440II, whereas KpMVS2 possessed unique
245 plasmid types IncFII/IncR and IncFII(pKP91)/FIB(K).

246 KpMVS1 carried $bla_{\text{KPC-2}}$ on the 111.4 kbp IncFII(pKP91)/repB(R1701) plasmid pKpMVS1_1. A
247 plasmid of the same type was identified in KpMVR1 (pKpMVR1_1, 111.2 kbp) and carried $bla_{\text{KPC-157}}$,
248 which differed from $bla_{\text{KPC-2}}$ by a single missense mutation (392A>G) resulting in an N131S amino
249 acid substitution within the enzyme's active site [58], where N131 bounds to relebactam, avibactam,
250 and vaborbactam through a hydrogen bond [59–61]. Notably, pKpMVR1_1 differed from
251 pKpMVS1_1 by 285 nucleotide substitutions, 14 deletions, and three insertions. These variants were
252 concentrated in two genomic regions involved in plasmid transfer and maintenance (Figure S1),
253 suggesting recombination between plasmids. Another plasmid type, IncFII(pKP91)/IncR, in KpMVS2
254 harboured $bla_{\text{KPC-2}}$. All these KPC-encoding plasmids were predicted to be conjugative (relaxase type:
255 MOBF; mating pair formation type: MPF_F), and each carried a variant of the Tn*4401a* transposon
256 harbouring $bla_{\text{KPC-2}}$ or $bla_{\text{KPC-157}}$, with 1–2 SNPs between each pair of transposons (Table S1, Figure
257 S1). The comparison between fold-coverages of contigs suggested that each of these three isolates
258 carried a single copy of the KPC-encoding plasmid. Other AMR genes detected in these isolates were
259 chromosomal β-lactamase gene bla_{SHV} (variant $bla_{\text{SHV-36}}$) and fosfomycin resistance gene *fosA10*,
260 which are both intrinsic to *K. pneumoniae* [62–64].

261 The chromosome of KpMVR1 differed from that of KpMVS1 by six single-nucleotide
262 polymorphisms (SNPs), seven insertions, and eight deletions (including four large deletions illustrated
263 in Figures 1 and S2–5). Seven of these genetic variants were also identified in KpMVS2 (Table 4),

264 which differed from KpMVS1 by 129 SNPs, 13 insertions, and seven deletions. Two large deletions
265 (19.7 kbp and 4.9 kbp) in KpMVR1 could be attributed to an IS-mediated deletion that had previously
266 been observed in *Escherichia coli* (Figures S3 and S5) [65]. Notably, KpMVR1 exhibited deletion of
267 a 54.7-kbp region that comprised operons producing an AcrAB-like multidrug efflux pump and an
268 additional ABC-type Fe^{3+}-siderophore transport system in both KpMVS1 and KpMVS2 (Figure 1 and
269 Table S2). Each of the three isolates carried a single copy of the *acrRAB* operon and *tolC* gene, which
270 combine to produce the AcrAB-TolC multidrug efflux pump. However, the permease AcrB in
271 KpMVR1 differed from that in KpMVS1 and KpMVS2 by a destabilising mutation L667R outside the
272 protein's transmembrane domains.

273 As for the biosynthesis of siderophores and transport of the iron-siderophore complex, which
274 facilitate cefiderocol to penetrate the OM [66], KpMVS1, KpMVR1, and KpMVS2 were predicted to
275 possess complete enterobactin production and iron-enterobactin transport systems, while none of the
276 yersiniabactin, colibactin, aerobactin, or salmochelin loci were detected, corresponding to a Kleborate
277 virulence score of zero. All three isolates shared the same 19-kbp chromosomal region harbouring a
278 cluster of enterobactin-synthesising genes *entA–F and entH*, enterobactin-exporter gene *entS*, and iron-
279 enterobactin transporter genes *fepA–D* and *fepG*.

280 Compared with the ciprofloxacin-susceptible isolates KpMVS1 and KpMVS2, KpMVR1
281 harboured a nucleotide substitution 248C>A in the DNA gyrase gene *gyrA*, resulting in the GyrA
282 mutation S83Y, which is known to reduce ciprofloxacin susceptibility [67]. The three isolates also
283 carried a single copy of the *marRAB* operon. However, KpMVR1 exhibited a unique 15-bp in-frame
284 deletion in the non-essential transcriptional repressor gene *marR* within the *marRAB* operon, causing
285 a loss of five amino acids and an amino acid substitution within the DNA-binding region of MarR
286 (Table 4) [68].

287 Seven bases at the 5' end of *ompK36* in KpMVR1 were truncated by an additional copy of insertion
288 sequence IS*Ec68* (three copies in KpMVS1 and KpMVS2, respectively), resulting in a frameshift

289 mutation that replaced the first three amino acids at the N-terminal of OmpK36 with 12 amino acids
290 (Figure 2). The native 21 N-terminal amino acids of OmpK36 encode a Sec-dependent signal sequence
291 (UniProtKB accession: A0A0H3H0Y2) that is required for translocating this protein to the inner
292 membrane of *K. pneumoniae* (Figure 2B) [69]. The signal sequence is subsequently cleaved and
293 OmpK36 is then folded and inserted into the OM (where the protein is functionally active as a porin)
294 in a Bam-complex dependent fashion, a process facilitated by a C-terminal recognition sequence [70].
295 Whilst *ompK36* from KpMVS1 and KpMVS2 is predicted to encode a complete sec-dependent signal
296 sequence, the 12 amino acids insertion combined with the deletion of three amino acids in OmpK36
297 from KpMVR1 is predicted to hinder this protein's translocation to the OM according to the disrupted
298 signal sequence (Figure S6). These predictions were confirmed by polyacrylamide gel electrophoresis
299 of OM preparations, followed by Coomassie staining, that a band corresponding to OmpK36 was
300 present in KpMVS1 but absent in KpMVR1 (Figure 2C). Therefore, the disruption of the Sec-
301 dependent signal sequence of OmpK36 is functionally equivalent to deletion of *ompK36*.

302 Regarding the plasmid-encoded TraN proteins, $TraN_{pKpMVR1_1}$ and $TraN_{pKpMVS2_1}$ were identical
303 (NCBI protein accession: WP_049192820.1) and differed from $TraN_{pKpMVS1_1}$ (WP_436914186.1) by
304 six amino acid substitutions (Table S6). Phylogenetic analysis revealed that these proteins belonged to
305 the specialist TraNβ group (Figure S7), which has a narrow host range [50, 71]. Pairwise structural
306 comparison between $TraN_{pKpMVR1_1}$ ($TraN_{pKpMVS2_1}$), $TraN_{pKpMVS1_1}$, and the prototype TraNβ protein
307 $TraN_{pKpQIL}$ showed high consistency (Figures S8), and no amino acid substitution occurred in the
308 characteristic distal β-hairpin (Figure S9), suggesting that the variation in TraN sequences across
309 plasmids pKpMVR1_1, pKpMVS1_1, pKpMVS2_1, and pKpQIL is unlikely to affect the conjugation
310 specificity [72].

311 **Impact of genetic alterations on antimicrobial resistance**

312 The substitution of bla_{KPC-2} with $bla_{KPC-157}$ in KpMVS1 ($KpMVS1_{KPC-157}$) and the transconjugant
313 $ICC8001_{KPC-2}$ ($ICC8001_{KPC-157}$) did not affect the susceptibility to meropenem, meropenem-

314 vaborbactam, or imipenem-avibactam but led to a fourfold reduction in the imipenem MIC and a 16-
315 to 32-fold increase in imipenem-relebactam MIC (Table 2). Moreover, this allelic substitution resulted
316 in a 256- to 512-fold reduction in the aztreonam MIC, a 32- to 64-fold reduction in the ceftazidime
317 MIC, and a ≥4-fold reduction in the cefiderocol MIC, but had no effect on the MICs of aztreonam-
318 avibactam or ceftazidime-avibactam. Notably, imipenem and imipenem-relebactam MICs of each
319 KPC-157-producing isolate were identical (Table 2). These findings suggest that KPC-157 has a
320 weaker capacity to hydrolyse imipenem, aztreonam, ceftazidime, and cefiderocol than KPC-2, and
321 that—unlike vaborbactam and avibactam, which inhibit both KPC variants—relebactam inhibits KPC-
322 2 but not KPC-157, which is consistent with a previous report [59].

323 Knocking out *ompK36* from the ICC8001 chromosome ($ICC8001_{KPC-2/\Delta ompK36}$ and $ICC8001_{KPC-}$
324 $_{157/\Delta ompK36}$) led to a 16-fold increase in the MICs of both meropenem and imipenem, a >33-fold increase
325 in the meropenem-vaborbactam MIC, an 8- to 32-fold increase in the imipenem-relebactam MIC, and
326 a more than twofold increase in the aztreonam MIC (Table 2). These findings are consistent with the
327 role of OmpK36 as an entry route for β-lactams and β-lactamase inhibitors to penetrate the OM [73].
328 Nevertheless, when comparing MICs of ceftazidime, ceftazidime-avibactam, and cefiderocol before
329 and after knocking out *ompK36* from $ICC8001_{KPC-2}$ and $ICC8001_{KPC-157}$, only two pairs of MICs
330 exhibited notable increases (from 0.125 mg/L to 0.5 mg/L for ceftazidime-avibactam, and from ≤0.06
331 mg/L to 0.25 mg/L for cefiderocol), while the others showed no appreciable changes, suggesting
332 alternative routes of avibactam's entry. More generally, the comparison between β-lactam MICs with
333 and without β-lactamase inhibitors for isolates KpMVR1, $ICC8001_{KPC-2/\Delta ompK36}$, and $ICC8001_{KPC-}$
334 $_{157/\Delta ompK36}$ in Table 2 indicates that these inhibitors penetrated the OM via routes other than OmpK36,
335 effectively inhibiting β-lactamases.

336 The chromosomes of KpMVR1, KpMVS1, and ICC8001 derivatives harboured the same cluster
337 of *ent* and *fep* genes within a 19-kbp region encoding an ABC-type Fe^{3+}-siderophore transporter
338 associated with the cefiderocol susceptibility [66]. These isolates did not exhibit any notable difference

339 in cefiderocol MICs despite KpMVR1's loss of the 54.7-kbp chromosomal region harbouring *fep*-like
340 genes (Table S2), suggesting alternative entry routes of cefiderocol.

341 Discussion

342 In the UK, meropenem-vaborbactam and imipenem-relebactam are recommended for treating adult
343 patients (≥18 years of age) with severe multidrug-resistant infections where therapeutic options are
344 limited, and ceftazidime-avibactam is recommended as an alternative when the disease-causing
345 bacterium produces class D carbapenemase (*e.g.*, OXA-48) [74–76]. Prevalence of resistance in
346 Enterobacterales to any of these three combination antimicrobials was 1–5% across the globe as of
347 2022 despite regional variation [17, 77–81]. Therefore, the discovery of *K. pneumoniae* isolate
348 KpMVR1, which exhibited unusual resistance to meropenem-vaborbactam, imipenem-relebactam,
349 and ceftazidime-avibactam, in a seriously ill patient is particularly worrisome. The small number of
350 chromosomal SNPs (n=6) and indels (n=10; ≤15 bp each) identified in KpMVR1 when compared with
351 KpMVS1, Patient 1's exposure to meropenem, meropenem-vaborbactam, and fluoroquinolones, and
352 the unique antibiogram of KpMVR1 in the ICU altogether support the suspected *in vivo* emergence of
353 meropenem-vaborbactam, ceftazidime-avibactam, imipenem-relebactam, and ciprofloxacin resistance
354 in the same *K. pneumoniae* strain during this patient's hospital stay. A similar shift in the ceftazidime-
355 avibactam susceptibility profile of *K. pneumoniae* has been reported during treatment using
356 meropenem followed by ceftazidime-avibactam [82].

357 KPC-2 is known to confer carbapenem resistance in Gram-negative bacteria but can be effectively
358 inhibited by vaborbactam, avibactam, and relebactam [83]. Here, we have experimentally determined
359 the effect of carbapenemase KPC-157 on the susceptibility to carbapenems and cephalosporins with
360 or without β-lactamase inhibitors. Our results indicate that KPC-157 does not differ from KPC-2 in its
361 interaction with meropenem or meropenem-vaborbactam. Therefore, the presence of $bla_{\text{KPC-157}}$ in the
362 single-copy plasmid pKpMVR1_1 alone cannot explain the high-level meropenem-vaborbactam

363 resistance observed in KpMVR1. Notably, KPC-157 appears less capable of hydrolysing imipenem,
364 aztreonam, ceftazidime, and cefiderocol than KPC-2, and is inhibited by vaborbactam and avibactam
365 but not by relebactam.

366 Isolate KpMVR1 showed genetic changes that may alter the antimicrobial permeability of its OM
367 when compared with isolate KpMVS1. Resulting from an IS-induced sequence disruption, the
368 hindered translocation of OmpK36 to the OM is predicted to hamper the influx of β-lactams and β-
369 lactamase inhibitors into the periplasm, hence elevated MICs of carbapenems and cephalosporins
370 tested in Table 2 with and without β-lactamase inhibitors. Such hampered antimicrobial and inhibitor
371 influx might be further compromised by a decreased expression of *ompK35* in KpMVR1 as a result of
372 the in-frame, presumptively inactivating deletion within the repressor gene *marR* and the consequent
373 upregulation of the *marA* gene [84]. Moreover, the inactivation of *marR* is known to increase the
374 production of the AcrAB-TolC efflux pump, conferring low-level cross-resistance to antimicrobials
375 including β-lactams and ciprofloxacin [85]. However, this upregulation of AcrAB-TolC in KpMVR1
376 might not alter its antimicrobial susceptibility owing to the possibly destabilised AcrB. Therefore, the
377 high-level ciprofloxacin resistance in KpMVR1 could be primarily driven by the combination of the
378 *gyrA* mutation S83Y and the absence of OmpK36 in this isolate's OM [67, 86].

379 This study is limited to three *K. pneumoniae* isolates belonging to the same clone, with only one
380 isolate (KpMVR1) exhibiting elevated MICs of meropenem-vaborbactam, imipenem-relebactam,
381 aztreonam-avibactam, and ceftazidime-avibactam. KpMVR1 harboured multiple AMR-associated
382 genetic alterations. Broader surveillance of genetic variants similar to those identified in KpMVR1 is
383 needed to assess the prevalence and clinical relevance of these putative resistance mechanisms.
384 Although we experimentally validated the individual contributions of $bla_{\text{KPC-157}}$ and Δ*ompK36* to
385 antimicrobial susceptibility, the genetically reconstructed isolates could not fully replicate the same
386 level of MIC increments as KpMVR1, suggesting that other genetic or regulatory mechanisms may be
387 involved, which remain to be elucidated. Transcriptomic and proteomic profiling could be performed

388 in the future to determine whether regulatory mechanisms also contribute to the observed AMR in
389 KpMVR1.

390 At the nation level, a review of routine surveillance and reference laboratory samples from 2016-
391 2020 revealed only low levels of resistance to ceftazidime-avibactam in the UK [81]. However, it
392 remains essential that emerging resistance to ceftazidime-avibactam and novel β-lactam/β-lactamase
393 inhibitor combinations is promptly identified and reported through UKHSA's Second Generation
394 Surveillance System and referral of such isolates to the AMRHAI Reference Unit. Additionally, our
395 study highlights the importance of monitoring the evolving antimicrobial susceptibility profiles of
396 bacterial pathogens within patients during antimicrobial therapy.

397 Funding information

398 This work was mainly funded by the UKHSA. YW is a research fellow funded by the David Price
399 Evans Endowment (grant number: UGG10057) at the University of Liverpool and was an Imperial
400 Institutional Strategic Support Fund Springboard Research Fellow, funded by the Wellcome Trust and
401 Imperial College London (grant number: PSN109). YW, EJ, DM, and KLH are affiliated with the
402 National Institute for Health and Care Research Health Protection Research Unit in Healthcare
403 Associated Infections and Antimicrobial Resistance at Imperial College London in partnership with
404 the UKHSA, in collaboration with, Imperial Healthcare Partners, University of Cambridge and
405 University of Warwick (grant number: NIHR200876). The views expressed in this article are those of
406 the authors and not necessarily those of the NHS, the National Institute for Health Research, or the
407 Department of Health and Social Care.

408 Acknowledgments

409 We acknowledge the Colebrook Laboratory, a facility supported by the NIHR Imperial Biomedical
410 Research Centre (BRC), for providing bioinformatics resources. Part of the bioinformatics analysis

411 was performed on equipment purchased as part of MRC CARP fellowship award MR/T005254/1. We
412 also thank the Institut Pasteur teams for the curation and maintenance of BIGSdb-Pasteur databases at
413 http://bigsdb.pasteur.fr.

414 Author contributions

415 Conceptualisation: KLH and YW; Resources: KLH, JT, GF, FM, NW, and GMR; Methodology: KLH,
416 YW, JLCW, and EJ; Data curation: YW; Investigation and formal analysis: YW, JLCW, JSG, WWL,
417 JT, FM, GMR, KD, IB, GF, EJ, DM, and KLH; Visualisation: YW; Writing – original draft: YW,
418 JLCW, JSG, WWL, GMR, and KLH; Writing – review and editing: all authors.

419 Conflicts of interest

420 Authors declare that there are no conflicts of interest.

421 Consent to publish

422 No sensitive information is disclosed in this manuscript.

423 Ethical statement

424 National surveillance of communicable diseases and outbreak investigation work at UKHSA does not
425 require individual patient consent as per Regulation 3 of The Health Service (Control of Patient
426 Information) Regulations 2002.

427 References

428 1. **Baldwin CM, Lyseng-Williamson KA, Keam SJ**. Meropenem. *Drugs* 2008;68:803–838.

429 2. **Meini S, Tascini C, Cei M, Sozio E, Rossolini GM**. AmpC β-lactamase-producing
430 Enterobacterales: what a clinician should know. *Infection* 2019;47:363–375.

431 3. **Livermore DM**. Defining an extended-spectrum β-lactamase. *Clinical Microbiology and*
432 *Infection* 2008;14:3–10.

433 4. **Tooke CL, Hinchliffe P, Bragginton EC, Colenso CK, Hirvonen VHA, *et al.*** β-Lactamases and
434 β-Lactamase Inhibitors in the 21st Century. *Journal of Molecular Biology* 2019;431:3472–3500.

435 5. **Jacoby GA**. AmpC β-Lactamases. *Clinical Microbiology Reviews* 2009;22:161–182.

436 6. **Jorgensen SCJ, Rybak MJ**. Meropenem and Vaborbactam: Stepping up the Battle against
437 Carbapenem-resistant Enterobacteriaceae. *Pharmacotherapy: The Journal of Human*
438 *Pharmacology and Drug Therapy* 2018;38:444–461.

439 7. **Rodloff AC, Goldstein EJC, Torres A**. Two decades of imipenem therapy. *Journal of*
440 *Antimicrobial Chemotherapy* 2006;58:916–929.

441 8. **Prajapati JD, Kleinekathöfer U, Winterhalter M**. How to Enter a Bacterium: Bacterial Porins
442 and the Permeation of Antibiotics. *Chem Rev* 2021;121:5158–5192.

443 9. **Lomovskaya O, Sun D, Rubio-Aparicio D, Nelson K, Tsivkovski R, *et al.*** Vaborbactam:
444 Spectrum of Beta-Lactamase Inhibition and Impact of Resistance Mechanisms on Activity in
445 Enterobacteriaceae. *Antimicrobial Agents and Chemotherapy* 2017;61:10.1128/aac.01443-17.

446 10. **Ehmann DE, Jahić H, Ross PL, Gu R-F, Hu J, *et al.*** Kinetics of Avibactam Inhibition against
447 Class A, C, and D β-Lactamases. *Journal of Biological Chemistry* 2013;288:27960–27971.

448 11. **Carcione D, Siracusa C, Sulejmani A, Leoni V, Intra J**. Old and New Beta-Lactamase Inhibitors:
449 Molecular Structure, Mechanism of Action, and Clinical Use. *Antibiotics* 2021;10:995.

450 12. **UK Health Security Agency**. UK Access, Watch, Reserve, and Other classification for antibiotics
451 (UK-AWaRe antibiotic classification). https://www.gov.uk/government/publications/uk-aware-
452 antibiotic-classification/uk-access-watch-reserve-and-other-classification-for-antibiotics-uk-
453 aware-antibiotic-classification (2025).

454 13. **Sun D, Rubio-Aparicio D, Nelson K, Dudley MN, Lomovskaya O**. Meropenem-Vaborbactam
455 Resistance Selection, Resistance Prevention, and Molecular Mechanisms in Mutants of KPC-
456 Producing *Klebsiella pneumoniae*. *Antimicrobial Agents and Chemotherapy* 2017;61:e01694-17.

457 14. **Gaibani P, Bovo F, Bussini L, Lazzarotto T, Amadesi S, *et al.*** Dynamic evolution of
458 imipenem/relebactam resistance in a KPC-producing *Klebsiella pneumoniae* from a single patient
459 during ceftazidime/avibactam-based treatments. *Journal of Antimicrobial Chemotherapy*
460 2022;77:1570–1577.

461 15. **Gaibani P, Re MC, Campoli C, Viale PL, Ambretti S**. Bloodstream infection caused by KPC-
462 producing *Klebsiella pneumoniae* resistant to ceftazidime/avibactam: epidemiology and genomic
463 characterization. *Clinical Microbiology and Infection* 2020;26:516.e1-516.e4.

464 16. **Satapoomin Naphat, Dulyayangkul Punyawee, Avison Matthew B.** *Klebsiella pneumoniae*
465 Mutants Resistant to Ceftazidime-Avibactam Plus Aztreonam, Imipenem-Relebactam,
466 Meropenem-Vaborbactam, and Cefepime-Taniborbactam. *Antimicrobial Agents and*
467 *Chemotherapy* 2022;66:e02179-21.

468 17. **Gaibani P, Giani T, Bovo F, Lombardo D, Amadesi S, *et al.*** Resistance to
469 Ceftazidime/Avibactam, Meropenem/Vaborbactam and Imipenem/Relebactam in Gram-Negative
470 MDR Bacilli: Molecular Mechanisms and Susceptibility Testing. *Antibiotics* 2022;11:628.

471 18. **Gaibani Paolo, Bianco Gabriele, Amadesi Stefano, Boattini Matteo, Ambretti Simone, *et al.***
472 Increased *bla*$_{KPC}$ Copy Number and OmpK35 and OmpK36 Porins Disruption Mediated
473 Resistance to Imipenem/Relebactam and Meropenem/Vaborbactam in a KPC-Producing
474 *Klebsiella pneumoniae* Clinical Isolate. *Antimicrobial Agents and Chemotherapy*
475 2022;66:e00191-22.

476 19. **Wilson WR, Kline EG, Jones CE, Morder KT, Mettus RT, *et al.*** Effects of KPC Variant and
477 Porin Genotype on the In Vitro Activity of Meropenem-Vaborbactam against Carbapenem-
478 Resistant Enterobacteriaceae. *Antimicrobial Agents and Chemotherapy*
479 2019;63:10.1128/aac.02048-18.

480 20. **Humphries Romney M., Hemarajata Peera**. Resistance to Ceftazidime-Avibactam in *Klebsiella*
481 *pneumoniae* Due to Porin Mutations and the Increased Expression of KPC-3. *Antimicrobial Agents*
482 *and Chemotherapy* 2017;61:10.1128/aac.00537-17.

483 21. **Turton JF, Payne Z, Coward A, Hopkins KL, Turton JA, *et al.*** Virulence genes in isolates of
484 *Klebsiella pneumoniae* from the UK during 2016, including among carbapenemase gene-positive
485 hypervirulent K1-ST23 and 'non-hypervirulent' types ST147, ST15 and ST383. *Journal of*
486 *Medical Microbiology* 2018;67:118–128.

487 22. **The European Committee on Antimicrobial Susceptibility Testing**. Clinical breakpoints (v
488 15.0).
489 https://www.eucast.org/fileadmin/src/media/PDFs/EUCAST_files/Breakpoint_tables/v_15.0_Bre
490 akpoint_Tables.xlsx (2025).

491 23. **Bolger AM, Lohse M, Usadel B**. Trimmomatic: a flexible trimmer for Illumina sequence data.
492 *Bioinformatics* 2014;30:2114–2120.

493 24. **Chen S, Zhou Y, Chen Y, Gu J**. fastp: an ultra-fast all-in-one FASTQ preprocessor.
494 *Bioinformatics* 2018;34:i884–i890.

495 25. **Wood DE, Lu J, Langmead B**. Improved metagenomic analysis with Kraken 2. *Genome Biology*
496 2019;20:257.

497 26. **Lu J, Breitwieser FP, Thielen P, Salzberg SL**. Bracken: Estimating species abundance in
498 metagenomics data. *PeerJ Computer Science* 2017;2017:e104.

499 27. **Bouras G, Houtak G, Wick RR, Mallawaarachchi V, Roach MJ, *et al.*** Hybracter: Enabling
500 Scalable, Automated, Complete and Accurate Bacterial Genome Assemblies.
501 2023;2023.12.12.571215.

502 28. **Bouras G, Sheppard AE, Mallawaarachchi V, Vreugde S**. Plassembler: an automated bacterial
503 plasmid assembly tool. *Bioinformatics* 2023;39:btad409.

504 29. **Bouras G, Grigson SR, Papudeshi B, Mallawaarachchi V, Roach MJ**. Dnaapler: A tool to
505 reorient circular microbial genomes. *Journal of Open Source Software* 2024;9:5968.

506 30. Medaka. github.com/nanoporetech/medaka.

31. **Bouras G**. pypolca. https://github.com/gbouras13/pypolca (2024, accessed 29 February 2024).

32. **Wick RR, Holt KE**. Polypolish: Short-read polishing of long-read bacterial genome assemblies. *PLOS Computational Biology* 2022;18:e1009802.

33. **Chklovski A, Parks DH, Woodcroft BJ, Tyson GW**. CheckM2: a rapid, scalable and accurate tool for assessing microbial genome quality using machine learning. *Nature Methods* 2023;20:1203–1212.

34. **Pedersen BS, Quinlan AR**. Mosdepth: quick coverage calculation for genomes and exomes. *Bioinformatics* 2018;34:867–868.

35. **Schwengers O, Jelonek L, Dieckmann MA, Beyvers S, Blom J, *et al.*** Bakta: rapid and standardized annotation of bacterial genomes via alignment-free sequence identification. *Microbial Genomics* 2021;7:000685.

36. **Lam MMC, Wick RR, Watts SC, Cerdeira LT, Wyres KL, *et al.*** A genomic surveillance framework and genotyping tool for *Klebsiella pneumoniae* and its related species complex. *Nature Communications* 2021;12:4188.

37. **Wyres KL, Wick RR, Gorrie C, Jenney A, Follador R, *et al.*** Identification of *Klebsiella* capsule synthesis loci from whole genome data. *Microbial Genomics* 2016;2:e000102.

38. **Feldgarden M, Brover V, Gonzalez-Escalona N, Frye JG, Haendiges J, *et al.*** AMRFinderPlus and the Reference Gene Catalog facilitate examination of the genomic links among antimicrobial resistance, stress response, and virulence. *Sci Rep* 2021;11:12728.

39. **Couvin D, Bernheim A, Toffano-Nioche C, Touchon M, Michalik J, *et al.*** CRISPRCasFinder, an update of CRISRFinder, includes a portable version, enhanced performance and integrates search for Cas proteins. *Nucleic Acids Research* 2018;46:W246–W251.

40. **Carattoli A, Zankari E, García-Fernández A, Voldby Larsen M, Lund O, *et al.*** *In Silico* Detection and Typing of Plasmids using PlasmidFinder and Plasmid Multilocus Sequence Typing. *Antimicrobial Agents and Chemotherapy* 2014;58:3895–3903.

41. **Robertson J, Nash JHE**. MOB-suite: software tools for clustering, reconstruction and typing of plasmids from draft assemblies. *Microbial Genomics*;4. Epub ahead of print 2018. DOI: https://doi.org/10.1099/mgen.0.000206.

42. **Ross Karen, Varani Alessandro M., Snesrud Erik, Huang Hongzhan, Alvarenga Danillo Oliveira, *et al.*** TnCentral: a Prokaryotic Transposable Element Database and Web Portal for Transposon Analysis. *mBio* 2021;12:10.1128/mbio.02060-21.

43. **Siguier P, Perochon J, Lestrade L, Mahillon J, Chandler M**. ISfinder: the reference centre for bacterial insertion sequences. *Nucleic Acids Research* 2006;34:D32–D36.

44. **Li H**. Minimap2: pairwise alignment for nucleotide sequences. *Bioinformatics* 2018;34:3094–3100.

45. **Cingolani P, Platts A, Wang LL, Coon M, Nguyen T, *et al.*** A program for annotating and predicting the effects of single nucleotide polymorphisms, SnpEff. *Fly* 2012;6:80–92.

544 46. **Jones P, Binns D, Chang H-Y, Fraser M, Li W, *et al.*** InterProScan 5: genome-scale protein
545 function classification. *Bioinformatics* 2014;30:1236–1240.

546 47. **Ittisoponpisan S, Islam SA, Khanna T, Alhuzimi E, David A, *et al.*** Can Predicted Protein 3D
547 Structures Provide Reliable Insights into whether Missense Variants Are Disease Associated?
548 *Journal of Molecular Biology* 2019;431:2197–2212.

549 48. **The UniProt Consortium**. UniProt: a worldwide hub of protein knowledge. *Nucleic Acids*
550 *Research* 2019;47:D506–D515.

551 49. **Zhou Y, Pan Q, Pires DEV, Rodrigues CHM, Ascher DB**. DDMut: predicting effects of
552 mutations on protein stability using deep learning. *Nucleic Acids Research* 2023;51:W122–W128.

553 50. **Low WW, Wong JLC, Beltran LC, Seddon C, David S, *et al.*** Mating pair stabilization mediates
554 bacterial conjugation species specificity. *Nature Microbiology* 2022;7:1016–1027.

555 51. **Alikhan N-F, Petty NK, Ben Zakour NL, Beatson SA**. BLAST Ring Image Generator (BRIG):
556 simple prokaryote genome comparisons. *BMC Genomics* 2011;12:402.

557 52. **Grant JR, Enns E, Marinier E, Mandal A, Herman EK, *et al.*** Proksee: in-depth
558 characterization and visualization of bacterial genomes. *Nucleic Acids Research* 2023;51:W484–
559 W492.

560 53. **Wilkins D, Kurtz Z**. gggenes. wilkox.org/gggenes.

561 54. **Wong JLC, Romano M, Kerry LE, Kwong H-S, Low W-W, *et al.*** OmpK36-mediated
562 Carbapenem resistance attenuates ST258 *Klebsiella pneumoniae in vivo*. *Nature Communications*
563 2019;10:3957.

564 55. **Teufel F, Almagro Armenteros JJ, Johansen AR, Gíslason MH, Pihl SI, *et al.*** SignalP 6.0
565 predicts all five types of signal peptides using protein language models. *Nat Biotechnol*
566 2022;40:1023–1025.

567 56. **The European Committee on Antimicrobial Susceptibility Testing**. MIC determination of non-
568 fastidious and fastidious organisms. https://www.eucast.org/ast_of_bacteria/mic_determination.

569 57. **The European Committee on Antimicrobial Susceptibility Testing**. Guidance document on
570 broth microdilution testing of cefiderocol.
571 https://www.eucast.org/fileadmin/src/media/PDFs/EUCAST_files/Guidance_documents/Cefider
572 ocol_MIC_testing_EUCAST_guidance_document_January_2024.pdf (2024).

573 58. **Ke W, Bethel CR, Thomson JM, Bonomo RA, van den Akker F**. Crystal Structure of KPC-2:
574 Insights into Carbapenemase Activity in Class A β-Lactamases. *Biochemistry* 2007;46:5732–5740.

575 59. **Gato E, Guijarro-Sánchez P, Alonso-García I, Pedraza-Merino R, Conde A, *et al.*** *In vitro*
576 development of imipenem/relebactam resistance in KPC-producing *Klebsiella pneumoniae*
577 involves multiple mutations including OmpK36 disruption and KPC modification. *International*
578 *Journal of Antimicrobial Agents* 2023;62:106935.

579 60. **Krishnan NP, Nguyen NQ, Papp-Wallace KM, Bonomo RA, van den Akker F**. Inhibition of
580 *Klebsiella* β-Lactamases (SHV-1 and KPC-2) by Avibactam: A Structural Study. *PLOS ONE*
581 2015;10:e0136813.

582 61. **Pemberton Orville A., Tsivkovski Ruslan, Totrov Maxim, Lomovskaya Olga, Chen Yu**.
583 Structural Basis and Binding Kinetics of Vaborbactam in Class A β-Lactamase Inhibition.
584 *Antimicrobial Agents and Chemotherapy* 2020;64:10.1128/aac.00398-20.

585 62. **Holt KE, Wertheim H, Zadoks RN, Baker S, Whitehouse CA, *et al.*** Genomic analysis of
586 diversity, population structure, virulence, and antimicrobial resistance in *Klebsiella pneumoniae*,
587 an urgent threat to public health. *Proceedings of the National Academy of Sciences*. Epub ahead
588 of print 2015. DOI: 10.1073/pnas.1501049112.

589 63. **Tsang KK, Lam MMC, Wick RR, Wyres KL, Bachman M, *et al.*** Diversity, functional
590 classification and genotyping of SHV β-lactamases in *Klebsiella pneumoniae*.
591 2024;2024.04.05.587953.

592 64. **Huang Y, Lin Q, Zhou Q, Lv L, Wan M, *et al.*** Identification of *fosA10*, a Novel Plasmid-
593 Mediated Fosfomycin Resistance Gene of *Klebsiella pneumoniae* Origin, in *Escherichia coli*. *IDR*
594 2020;13:1273–1279.

595 65. **Wan Y, Sabnis A, Mumin Z, Potterill I, Jauneikaite E, *et al.*** IS*1*-related large-scale deletion of
596 chromosomal regions harbouring the oxygen-insensitive nitroreductase gene *nfsB* causes
597 nitrofurantoin heteroresistance in *Escherichia coli*. *Microbial Genomics* 2023;9:001102.

598 66. **Sato T, Yamawaki K**. Cefiderocol: Discovery, Chemistry, and *In Vivo* Profiles of a Novel
599 Siderophore Cephalosporin. *Clinical Infectious Diseases* 2019;69:S538–S543.

600 67. **Chen F-J, Lauderdale T-L, Ho M, Lo H-J**. The Roles of Mutations in *gyrA*, *parC*, and *ompK35*
601 in Fluoroquinolone Resistance in *Klebsiella pneumoniae*. *Microbial Drug Resistance* 2003;9:265–
602 271.

603 68. **Praski Alzrigat L, Huseby DL, Brandis G, Hughes D**. Fitness cost constrains the spectrum of
604 marR mutations in ciprofloxacin-resistant *Escherichia coli*. *Journal of Antimicrobial*
605 *Chemotherapy* 2017;72:3016–3024.

606 69. **Mori H, Ito K**. The Sec protein-translocation pathway. *Trends in Microbiology* 2001;9:494–500.

607 70. **Malinverni Juliana C., Silhavy Thomas J.** Assembly of Outer Membrane β-Barrel Proteins: the
608 Bam Complex. *EcoSal Plus* 2011;4:10.1128/ecosalplus.4.3.8.

609 71. **Frankel G, David S, Low WW, Seddon C, Wong JLC, *et al.*** Plasmids pick a bacterial partner
610 before committing to conjugation. *Nucleic Acids Res* 2023;51:8925–8933.

611 72. **Low Wen Wen, Seddon Chloe, Beis Konstantinos, Frankel Gad**. The Interaction of the F-Like
612 Plasmid-Encoded TraN Isoforms with Their Cognate Outer Membrane Receptors. *Journal of*
613 *Bacteriology* 2023;205:e00061-23.

614 73. **Rocker A, Lacey JA, Belousoff MJ, Wilksch JJ, Strugnell RA, *et al.*** Global Trends in Proteome
615 Remodeling of the Outer Membrane Modulate Antimicrobial Permeability in *Klebsiella*
616 *pneumoniae*. *mBio* 2020;11:10.1128/mbio.00603-20.

617 74. **National Institute for Health and Care Excellence**. Antimicrobial prescribing: meropenem with
618 vaborbactam (Evidence summary [ES21]). *National Institute for Health and Care Excellence*
619 *(NICE)*. https://www.nice.org.uk/advice/es21/chapter/Key-messages (2019).

620 75. **National Institute for Health and Care Excellence**. Ceftazidime with avibactam for treating
621 severe drug-resistant gram-negative bacterial infections (Health technology evaluation [HTE1]).
622 *National Institute for Health and Care Excellence (NICE)*.
623 https://www.nice.org.uk/guidance/hte1/chapter/1-Recommendations (2022).

624 76. **National Institute for Health and Care Excellence**. Antimicrobial prescribing: imipenem with
625 cilastatin and relebactam (Evidence summary [ES30]). *National Institute for Health and Care*
626 *Excellence (NICE)*. https://www.nice.org.uk/advice/es30/evidence (2020).

627 77. **Xu T, Guo Y, Ji Y, Wang B, Zhou K**. Epidemiology and Mechanisms of Ceftazidime–Avibactam
628 Resistance in Gram-Negative Bacteria. *Engineering* 2022;11:138–145.

629 78. **Sader HS, Mendes RE, Duncan L, Kimbrough JH, Carvalhaes CG, *et al.*** Ceftazidime-
630 avibactam, meropenem-vaborbactam, and imipenem-relebactam activities against multidrug-
631 resistant Enterobacterales from United States Medical Centers (2018–2022). *Diagnostic*
632 *Microbiology and Infectious Disease* 2023;106:115945.

633 79. **Hernández-García Marta, García-Castillo María, Bou Germán, Cercenado Emilia, Delgado-**
634 **Valverde Mercedes, *et al.*** Imipenem-Relebactam Susceptibility in Enterobacterales Isolates
635 Recovered from ICU Patients from Spain and Portugal (SUPERIOR and STEP Studies).
636 *Microbiology Spectrum* 2022;10:e02927-22.

637 80. **Shoulders BR, Casapao AM, Venugopalan V**. An Update on Existing and Emerging Data for
638 Meropenem-Vaborbactam. *Clinical Therapeutics* 2020;42:692–702.

639 81. **Guy RL, Hopkins KL, Budd EL, Wilson K, Fountain H, *et al.*** The importance of monitoring a
640 new antibiotic: ceftazidime/avibactam usage and resistance experience from England, 2016 to
641 2020. *Eurosurveillance* 2025;30:2400399.

642 82. **Sauerborn E, Corredor NC, Reska T, Perlas A, Vargas da Fonseca Atum S, *et al.*** Detection
643 of hidden antibiotic resistance through real-time genomics. *Nature Communications* 2024;15:5494.

644 83. **Theuretzbacher U, Carrara E, Conti M, Tacconelli E**. Role of new antibiotics for KPC-
645 producing *Klebsiella pneumoniae*. *Journal of Antimicrobial Chemotherapy* 2021;76:i47–i54.

646 84. **Sulavik MC, Gambino LF, Miller PF**. The MarR Repressor of the Multiple Antibiotic Resistance
647 (*mar*) Operon in *Escherichia coli*: Prototypic Member of a Family of Bacterial Regulatory Proteins
648 Involved in Sensing Phenolic Compounds. *Mol Med* 1995;1:436–446.

649 85. **Randall LP, Woodward MJ**. The multiple antibiotic resistance (*mar*) locus and its significance.
650 *Research in Veterinary Science* 2002;72:87–93.

651 86. **Martínez-Martínez L, Hernández-Allés S, Albertí S, Tomás J M, Benedi V J, *et al.*** *In vivo*
652 selection of porin-deficient mutants of *Klebsiella pneumoniae* with increased resistance to
653 cefoxitin and expanded-spectrum-cephalosporins. *Antimicrobial Agents and Chemotherapy*
654 1996;40:342–348.

655

Figures

Figure 1. Genetic structure of a 54.7-kbp region in KpMVS1 that was deleted in KpMVR1 (Table 4). Labels "start" and "end" indicate boundaries of the deleted region. Genes without known names are not labelled. Each asterisk indicates an allele from a named gene family.

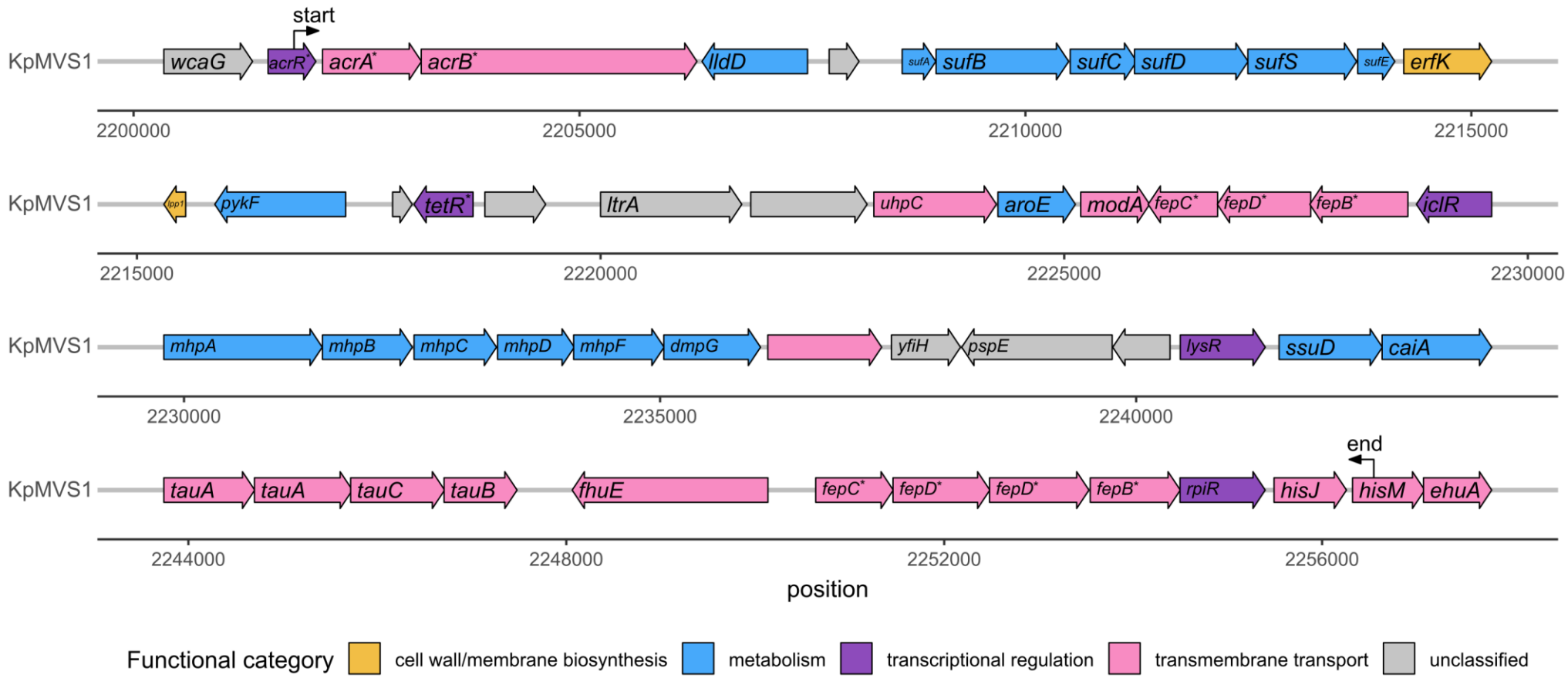

Figure 2. IS*Ec68*-mediated disruption of *ompK36* in isolate KpMVR1. (**A**) Genetic environment of the disrupted *ompK36* in KpMVR1. The arrow labelled "*ompK36**" denotes the upstream-shifted open reading frame caused by the insertion of IS*Ec68*. Abbreviations: CDS: coding sequence; IS, insertion sequence; ncRNA: non-coding RNA. (**B**) Comparison of predicted OmpK36 sequences using Clustal Omega (www.ebi.ac.uk/jdispatcher/msa/clustalo). Mismatches are highlighted in red, and the 22 N-terminal amino acids signal sequence of OmpK36 are indicated by the yellow shade. (**C**) Coomassie-stained polyacrylamide gel electrophoresis of outer membrane proteins to confirm the absence of OmpK36 in KpMVR1 and the *ompK36*-knockout isolate ICC8001$_{\Delta ompK36}$.

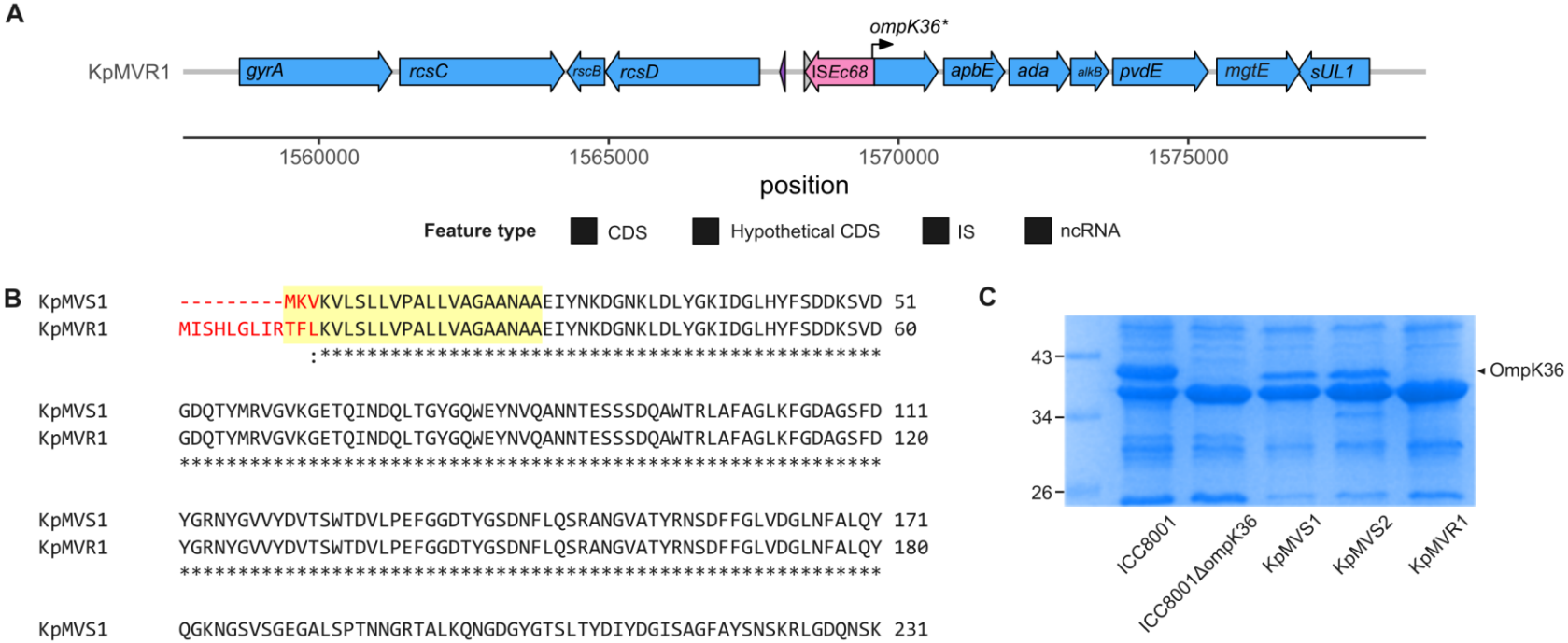

Supplementary methods

Genomic and molecular characterisation of a *Klebsiella pneumoniae* clinical isolate resistant to meropenem-vaborbactam, imipenem-relebactam, and ceftazidime-avibactam

Yu Wan, Joshua L. C. Wong, Julia Sanchez-Garrido, Wen Wen Low, Jane F. Turton, Fabio Morecchiato, Ilaria Baccani, Kirsty Dodgson, Gian Maria Rossolini, Neil Woodford, Gad Frankel, Elita Jauneikaite, Danièle Meunier, and Katie L. Hopkins

August 2025

Comparative structural analysis of TraN

Amino acid sequences of $TraN_{pKpMVS1_1}$, $TraN_{pKpMVR1_1}$, and $TraN_{pKpMVS2_1}$ were extracted from the sequence annotations of plasmids pKpMVS1_1 (locus tag: WAS92_RS00545), pKpMVR1_1 (ACNQKT_RS26595), and pKpMVS2_1 (ACNQKS_RS28350), respectively. To contextualise these three proteins, the previously described TraN variants [1] $TraN_{pKpQI}$ (NCBI protein accession: ARQ19727.1), $TraN_{MV2}$ (BAS44060.1), $TraN_{R100\text{-}1}$ (ABD60034.1), $TraN_{pSLT}$ (AAL23498.1), $TraN_{F}$ (WP_000821835.1), $TraN_{MV1}$ (ANZ89826.1), $TraN_{MV3}$ (WP_001398575.1) were downloaded from the NCBI Protein database (www.ncbi.nlm.nih.gov/protein). These 10 amino acid sequences were aligned with the ClustalW algorithm [2], and subsequently, a neighbour-joining phylogenetic tree was generated from the multi-sequence alignment, with the Poisson correction method as implemented in MEGA11 [3]. The phylogenetic tree was visualised using iTOL v7.2 [4].

Three-dimensional structures of $TraN_{pKpMVS1_1}$, $TraN_{pKpMVR1_1}$ (identical to $TraN_{pKpMVS2_1}$), and $TraN_{pKpQI}$ were predicted using AlphaFold 3 [5] with its default parameters on AlphaFold Server (alphafoldserver.com). The top-ranked (model 0) structural models of TraN proteins were visualised using UCSF ChimeraX v1.9 [6]. Superimposition analysis of these models was performed with ChimeraX's Matchmaker tool using default settings, including the use of the "best-aligning" or "bb" chain-pairing method, the Needleman-Wunsch alignment algorithm, and the BLOSUM-62 similarity matrix.

References

1. **Low Wen Wen, Seddon Chloe, Beis Konstantinos, Frankel Gad**. The Interaction of the F-Like Plasmid-Encoded TraN Isoforms with Their Cognate Outer Membrane Receptors. *Journal of Bacteriology* 2023;205:e00061-23.
2. **Thompson JD, Gibson TobyJ, Higgins DG**. Multiple Sequence Alignment Using ClustalW and ClustalX. *Current Protocols in Bioinformatics* 2003;00:2.3.1-2.3.22.
3. **Tamura K, Stecher G, Kumar S**. MEGA11: Molecular Evolutionary Genetics Analysis Version 11. *Molecular Biology and Evolution* 2021;38:3022–3027.
4. **Letunic I, Bork P**. Interactive Tree Of Life (iTOL): an online tool for phylogenetic tree display and annotation. *Bioinformatics* 2007;23:127–128.
5. **Abramson J, Adler J, Dunger J, Evans R, Green T, *et al.*** Accurate structure prediction of biomolecular interactions with AlphaFold 3. *Nature* 2024;630:493–500.
6. **Meng EC, Goddard TD, Pettersen EF, Couch GS, Pearson ZJ, *et al.*** UCSF ChimeraX: Tools for structure building and analysis. *Protein Science* 2023;32:e4792.

Supplementary figures

Genomic and molecular characterisation of a *Klebsiella pneumoniae* clinical isolate resistant to meropenem-vaborbactam, imipenem-relebactam, and ceftazidime-avibactam

Yu Wan, Joshua L. C. Wong, Julia Sanchez-Garrido, Wen Wen Low, Jane F. Turton, Fabio Morecchiato, Ilaria Baccani, Kirsty Dodgson, Gian Maria Rossolini, Neil Woodford, Gad Frankel, Elita Jauneikaite, Danièle Meunier, and Katie L. Hopkins

August 2025

Table of contents

Figure S1 1
Figure S2 2
Figure S3 3
Figure S4 4
Figure S5 4
Figure S6 5
Figure S7 6
Figure S8 7
Figure S9 8
Reference 9

Figure S1. Alignment of plasmids pKpMVR1_1 and pKpMVS2_1 against plasmid pKpMVS1_1 using nucleotide BLAST as implemented in Proksee. Plasmids pKpMVR1_1 and pKpMVS1_1 belonged to replicon type IncFII(pKP91)/repB(R1701), and pKpMVS2_1 belonged to IncFII(pKP91)/IncR. The innermost ring represents the number of genetic variants per kbp (calculated using VCFtools v0.1.17) [1] in pKpMVR2_1 compared with pKpMVS1_1. The two middle rings display genes, insertion sequences, and transposons identified in the reference sequence pKpMVS1_1, with arrows indicating orientations of these genetic features (Table S1). Genes without known names are not labelled. The two outer rings show regions of pKpMVR_1 (pink) and pKpMVS2_1 (blue) aligned to pKpMVS1, respectively. This figure was created using Proksee (proksee.ca). "Δ" in gene labels represents a truncated or interrupted feature, and each asterisk represents a variant of an insertion sequence or transposon. Abbreviations: CDS, coding sequence; IS, insertion sequence.

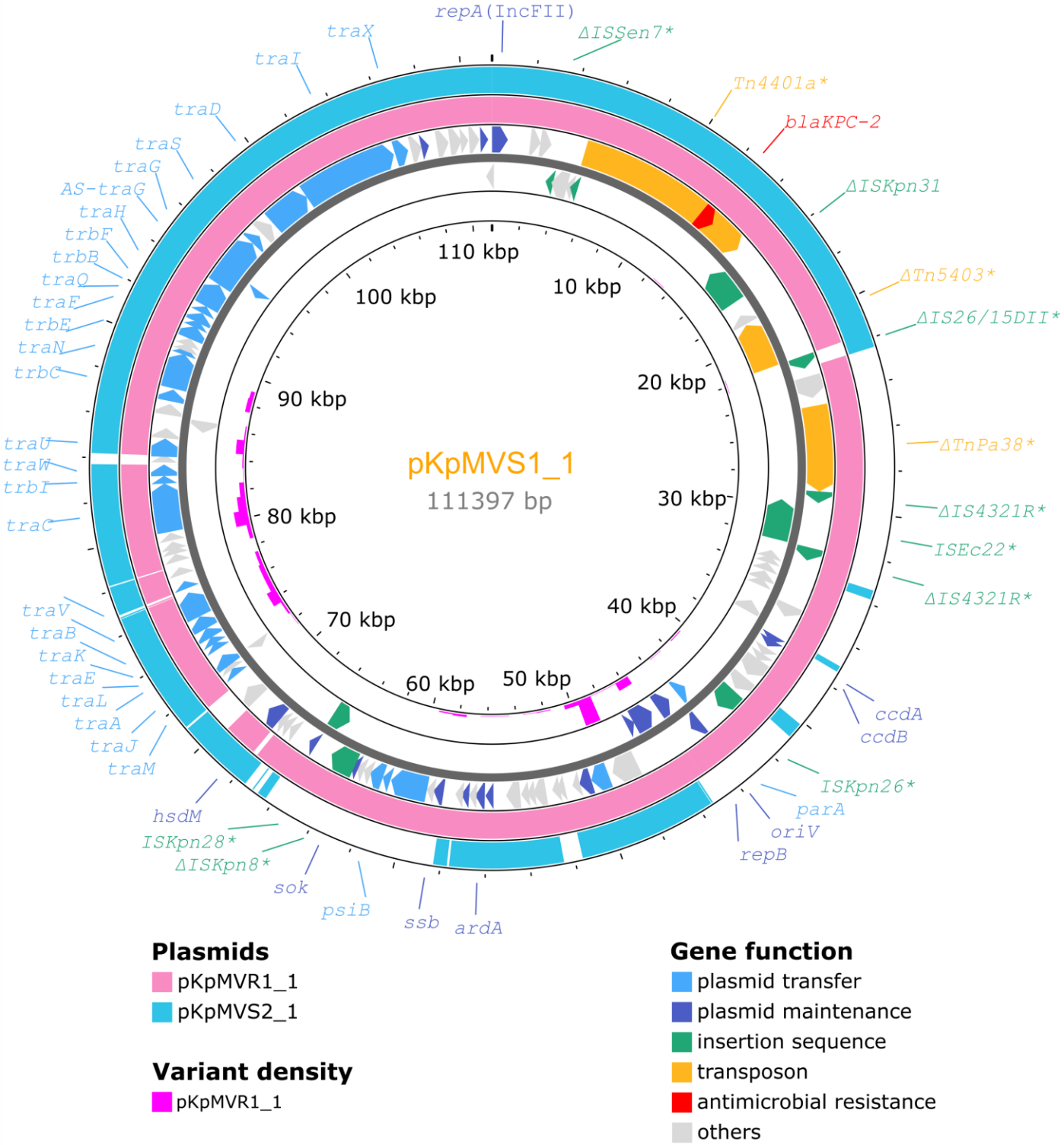

Figure S2. A BRIG diagram comparing chromosomes of KpMVR1 and KpMVS2 with that of KpMVS1. Parameters for BLASTn sequence alignment: "-task megablast -ungapped -qcov_hsp_perc 0.8". Four large deletions (>4 kbp) in the chromosome of KpMVR1 when compared to that of KpMVS1 (Table 3) are denoted by digits in filled circles. Genetic structures of these deleted regions are illustrated in Figure 1 and supplementary Figures S3–5.

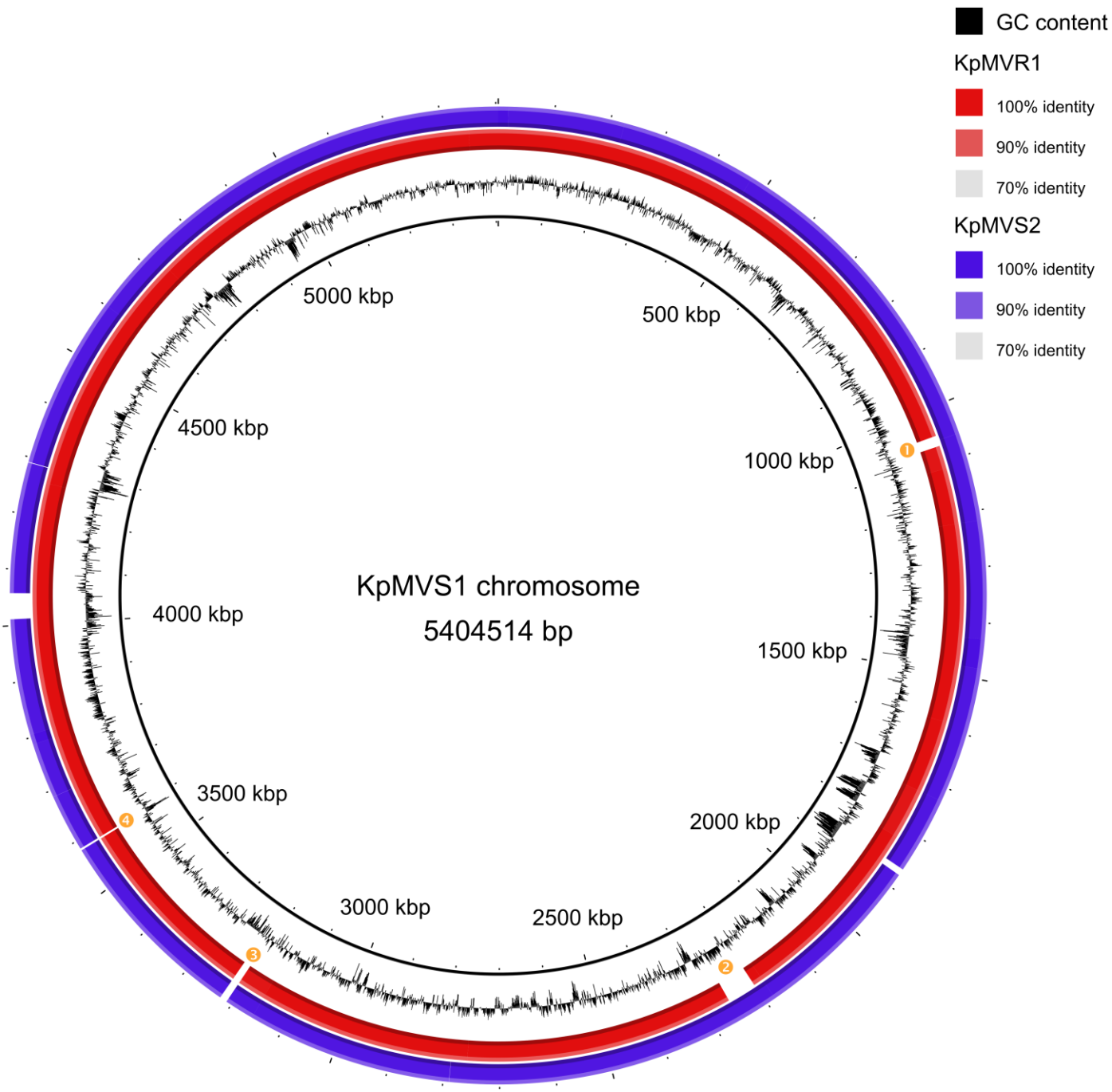

Figure S3. Genetic structure of a 19.7-kbp region in KpMVS1 that was deleted in KpMVR1 (Table 4). Labels "start" and "end" indicate boundaries of the deleted region. Genes without known names are not labelled. "IS*1X2**" denotes a variant of the IS*1*-family insertion sequence IS*1X2* (98% nucleotide identity and 100% query coverage). "CRISPR" indicates an array of clustered regularly interspaced short palindromic repeats. See Table S3 for detailed annotations of this region.

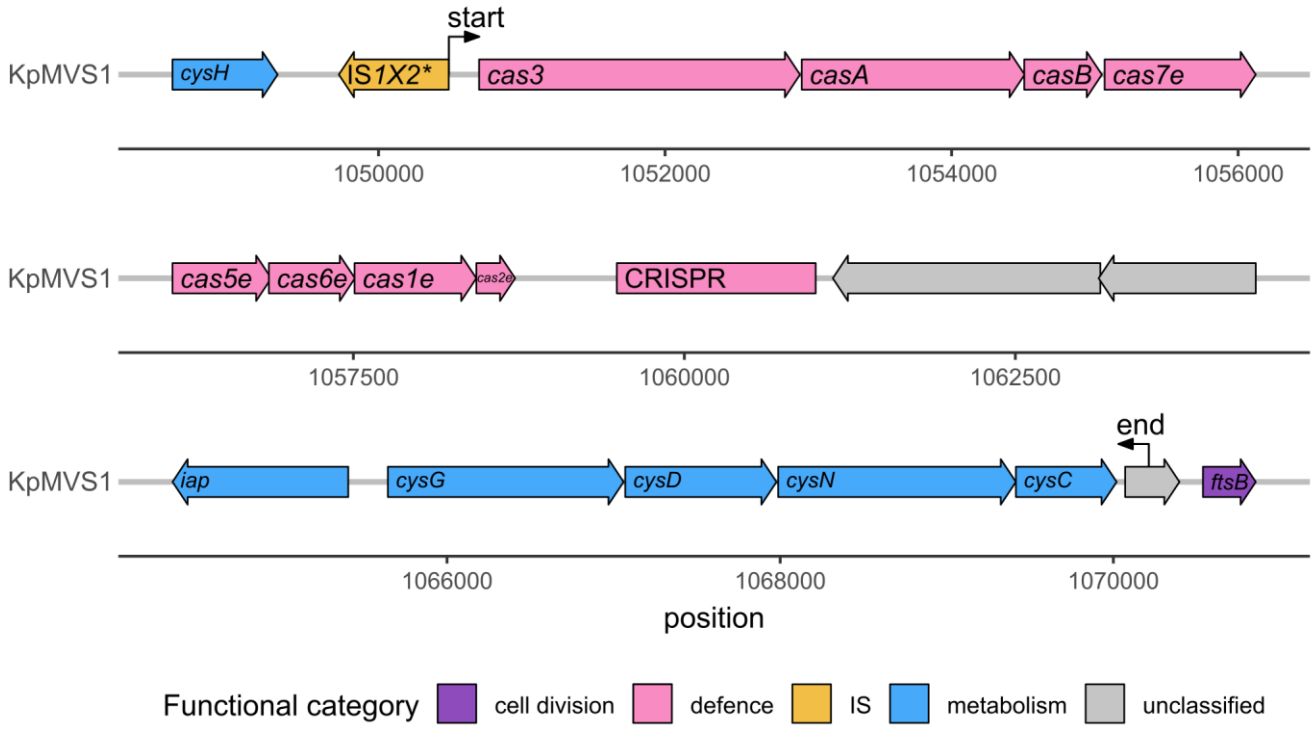

Figure S4. Genetic structure of a 33.5-kbp region in KpMVS1 that was deleted in KpMVR1 (Table 4). Labels "start" and "end" indicate boundaries of the deleted region. Genes without known names are not labelled. See Table S4 for detailed annotations of this region.

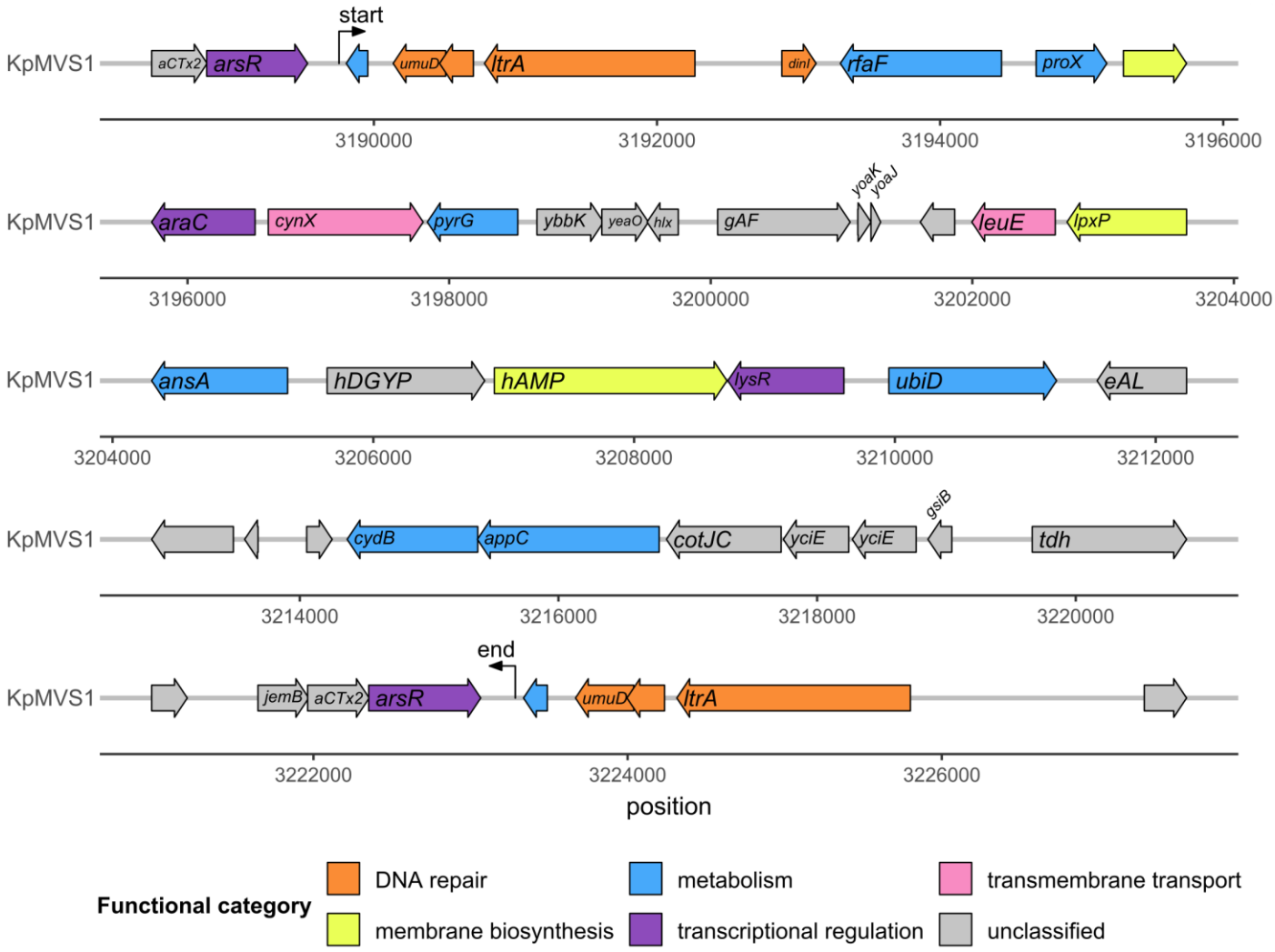

Figure S5. Genetic structure of a 4.9-kbp region in KpMVS1 that was deleted in KpMVR1 (Table 4). Labels "start" and "end" indicate boundaries of the deleted region. Genes without known names are not labelled. "IS*3H**" denotes a variant of the IS*3*-family insertion sequence IS*3H* (79% nucleotide identity and 100% query coverage). There were nine copies of this variant in the KpMVS1 chromosome and eight copies in the KpMVR1 chromosome, which is consistent with the content of the 4.9-kbp deletion (Table S5).

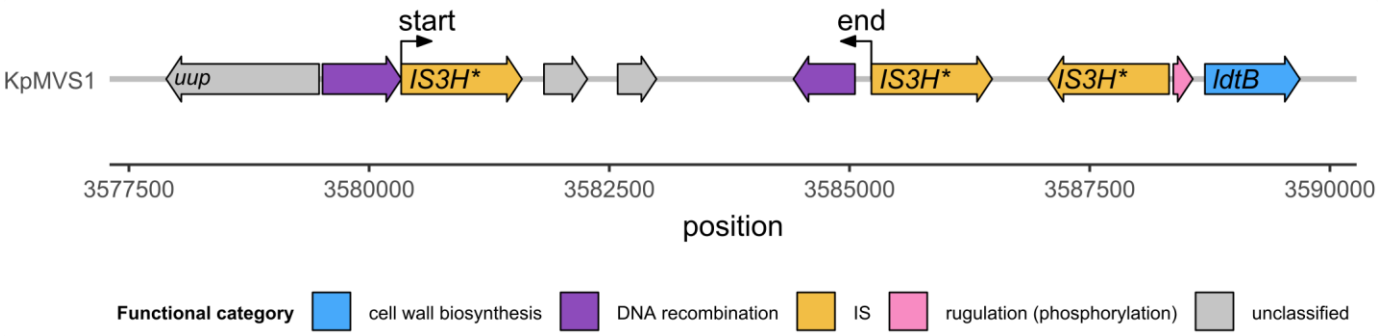

Figure S6. Prediction of signal peptides and cleavage site in the wild type OmpK36 (KpMVS1) and its frameshifted variant (KpMVR1), respectively, using the slow model mode of SignalP v6.0. "N", "H", and "C" regions in each protein sequence denote the N-terminal region (Sec/SPI n), centre hydrophobic region (Sec/SPI h), and C-terminal region (Sec/SPI c) of the signal peptide, respectively, whereas "O" denotes the non-signal peptide region (OTHER). The cleavage site (CS) is indicated by the red vertical dashed line. The probability of each amino acid to be part of each peptide region is indicated by a coloured solid curve throughout the protein sequence.

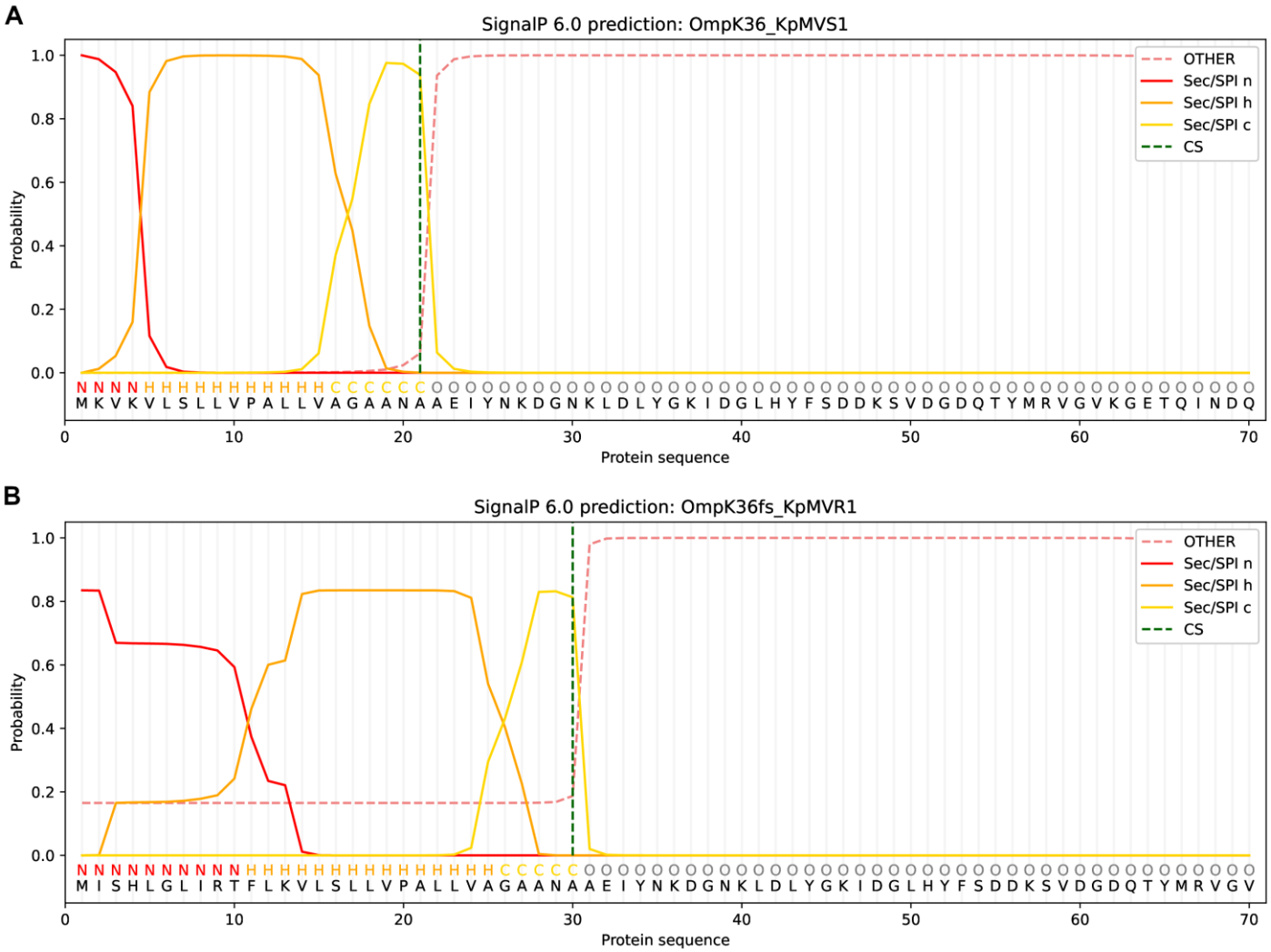
A
SignalP 6.0 prediction: OmpK36_KpMVS1
Probability
Protein sequence
OTHER
Sec/SPI n
Sec/SPI h
Sec/SPI c
CS
N N N N H H H H H H H H H H H H C C C C C C O O O

Figure S7. Midpoint-rooted neighbour-joining phylogenetic tree of 10 TraN amino acid sequences, where $TraN_{pKpMVR1_1}$ was identical to $Tra_{pKpMVS2_1}$. The sequences are named after source plasmids. The structural groups (TraNα, TraNβ, TraNγ, and TraNδ) [2] of TraN are indicated by shaded boxes and labelled. The scale bar represents the number of amino acid substitutions per residue.

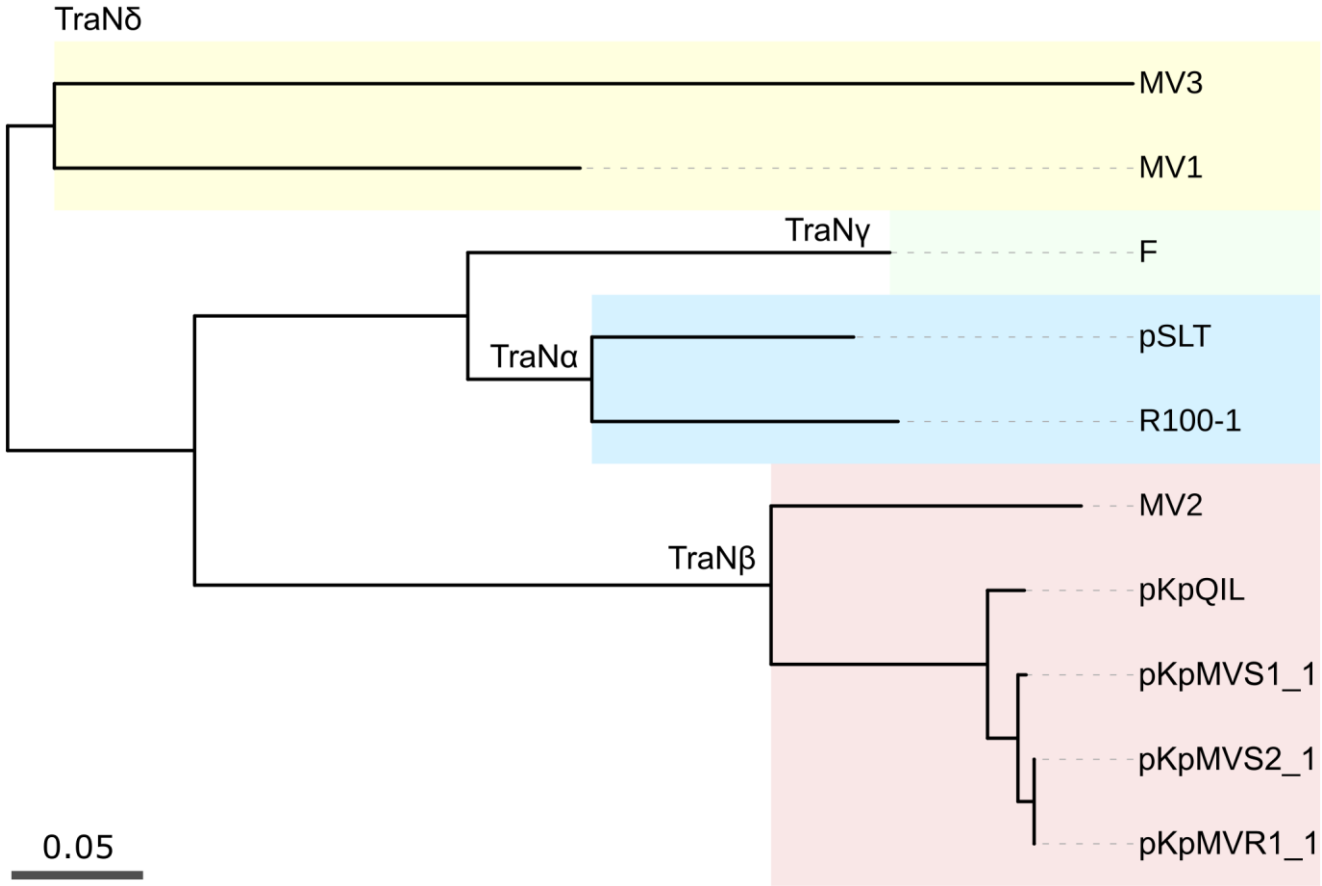

Figure S8. Comparison of predicted TraN structures for plasmids pKpQIL, pKpMVS1_1, and pKpMVR1_1. Amino acid chains are represented by ribbons. (**A**) Predicted 3D structures with residues coloured by scores from the predicted local distance difference test (pLDDT). The pLDDT was performed by AlphaFold3 to evaluate the per-residue local confidence of the predicted 3D structure. (**B**) Pairwise structural comparison through the super-imposition analysis. Dashed boxes indicate the tip/sensor domains of TraN [2].

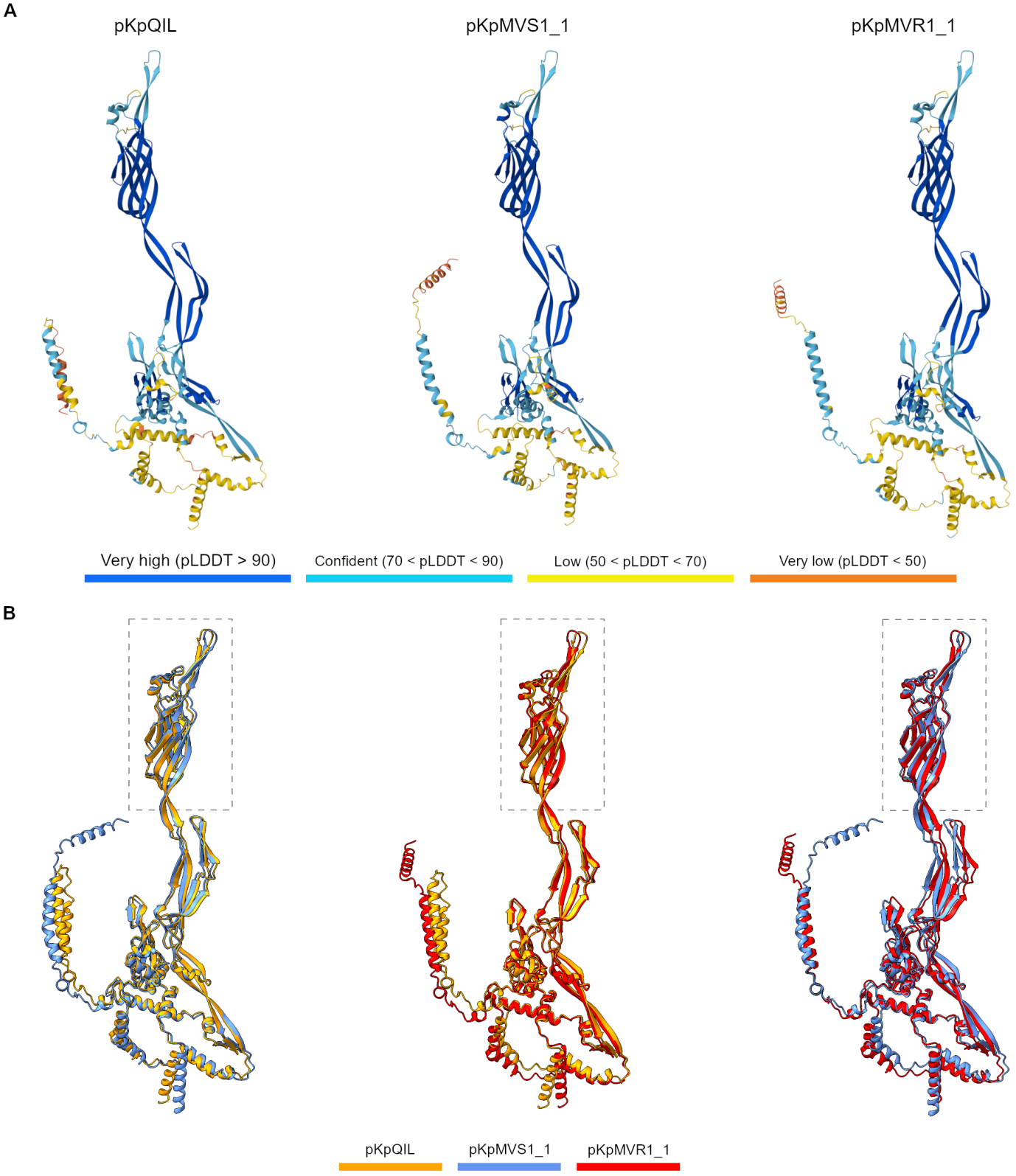

Figure S9. Locations of amino acid variation in the tip/sensor domains of TraN from plasmids pKpQIL, pKpMVS1_1, and pKpMVR1_1, with amino acid chains represented by ribbons in the superimposition view. The variable sites are highlighted in yellow, blue, and magenta. In comparison with Figure S8B, the proteins are arbitrarily rotated around the vertical axis to expose all variable sites.

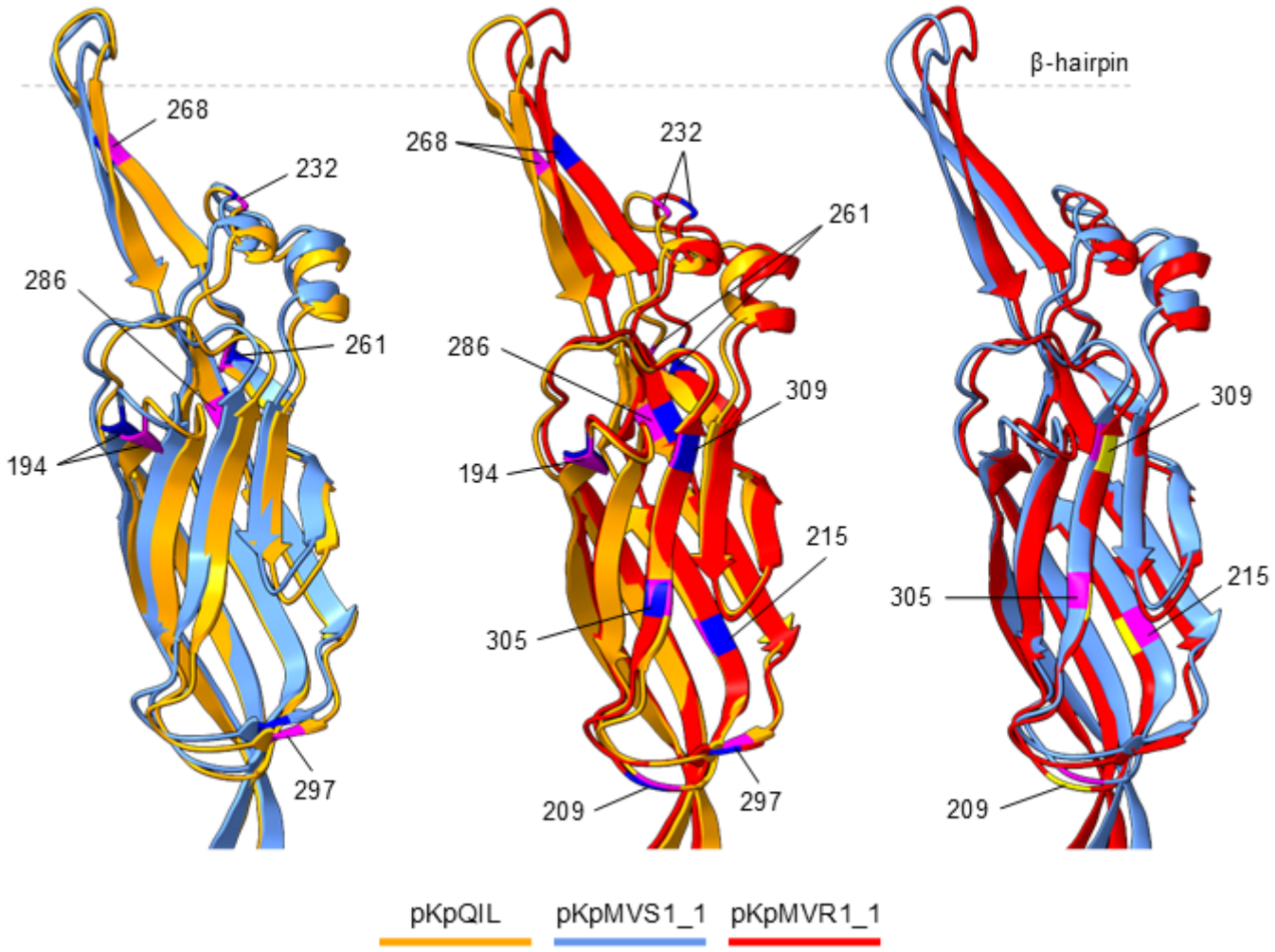

Reference

1. **Danecek P, Auton A, Abecasis G, Albers CA, Banks E, *et al.*** The variant call format and VCFtools. *Bioinformatics* 2011;27:2156–2158.

2. **Frankel G, David S, Low WW, Seddon C, Wong JLC, *et al.*** Plasmids pick a bacterial partner before committing to conjugation. *Nucleic Acids Res* 2023;51:8925–8933.